British Journal of Pharmacology (2004) 143, 303–317
www.nature.com/bjp

Pharmacological evidence for a key role of voltage-gated K^+ channels in the function of rat aortic smooth muscle cells

[1,2]Paolo Tammaro, [1]Amy L. Smith, [1,3]Simon R. Hutchings & *,[1]Sergey V. Smirnov

[1]Department of Pharmacy and Pharmacology, University of Bath, Claverton Down, Bath, BA2 7AY

1 The role of voltage-dependent (I_{K_v}) and large conductance Ca^{2+}-activated (BK_{Ca}) K^+ currents in the function of the rat aorta was investigated using specific BK_{Ca} and K_V channel inhibitors in single rat aortic myocytes (RAMs) with patch-clamp technique and in endothelium-denuded aortic rings with isometric tension measurements.

2 The whole-cell K^+ currents were recorded in RAMs dialysed with 200 and 444 nM Ca^{2+} and in perforated-patch configuration. Electrophysiological analysis demonstrated that I_{K_v} appeared at $\geqslant -40$ mV, while BK_{Ca} (isolated using 1 μM paxilline) were seen positive to -20 mV in all conditions.

3 Voltage-dependent characteristics, but not maximal conductance, of I_{K_v} was significantly altered in increased $[Ca^{2+}]_i$. Correolide (1 μM) (a K_V1 channel blocker) did not inhibit the I_{K_v}, whereas millimolar concentration of TEA ($IC_{50} = 3.1 \pm 0.6$ mM, $n = 5$) and 4-aminopyridine (4-AP, $IC_{50} = 5.9 \pm 1.9$ mM, $n = 7$) suppressed I_{K_v}. These results and immunocytochemical analysis suggest the $K_V2.1$ channel to be a molecular correlate for I_{K_v}.

4 In nonstimulated aortic rings 1–5 mM TEA and 4-AP (inhibitors of I_{K_v}), but not paxilline (1 μM), caused contraction. The frequency of contractile responses to TEA and 4-AP was increased in the presence of 10 mM KCl, which itself did not significantly affect the aortic basal tone.

5 Phenylephrine (15–40 nM) induced sustained tension with superimposed slow oscillatory contractions (termed OWs). OWs were blocked by diltiazem, ryanodine and cyclopiazonic acid, suggesting the involvement of L-type Ca^{2+} channels and ryanodine-sensitive Ca^{2+} stores in this process.

6 TEA and 4-AP, but not IbTX, paxilline or correolide, increased the duration and amplitude of OWs, indicating that I_{K_v} is involved in the control of oscillatory activity.

7 In conclusion, our findings suggest that the $K_V2.1$-mediated I_{K_v}, and not BK_{Ca}, plays an important role in the regulation of the excitability and contractility of rat aorta.
British Journal of Pharmacology (2004) **143,** 303–317. doi:10.1038/sj.bjp.0705957

Keywords: Vascular smooth muscle cells; potassium channels; single smooth muscle cells; patch-clamp technique; rhythmic contraction; thoracic aorta; rat; Ca^{2+}-activated K^+ channels; voltage-gated K^+ channels; $K_V2.1$ channel

Abbreviations: 4-AP, 4-aminopyridine; BK_{Ca}, large conductance Ca^{2+}-activated K^+ current; ChTX, charybdotoxin; C_m, cell membrane capacitance; CPA, cyclopiazonic acid; IbTX, iberiotoxin; I_{K_v}, voltage-dependent K^+ current; IP_3, inositol-1,4,5-triphosphate; k_a, slope factor of activation; k_h, slope factor of inactivation; K_V, voltage-dependent K^+ channel; L-VDCC, L-type voltage-dependent Ca^{2+} channel; OW, oscillatory wave of contraction; PE, phenylephrine; PP, perforated patch; PSS, physiological salt solution; RAM, rat aortic myocyte; SERCA, sarcoplasmic/endoplasmic reticulum Ca^{2+}-ATPase; TEA, tetraethylammonium; V_a, half-activation potential; V_h, half-inactivation potential; VSMC, vascular smooth muscle cell

Introduction

Potassium (K^+) channels play an important role in the regulation of the resting membrane potential and vascular contractility. Stimulation of vascular smooth muscle cells (VSMCs) with high K^+ or α_1-adrenoreceptor agonists causes membrane depolarisation and elevation of intracellular Ca^{2+} concentration ($[Ca^{2+}]_i$), resulting in contraction and a reduction of vessel diameter. Ca^{2+} entry *via* L-type voltage-dependent Ca^{2+} channels (L-VDCCs), activated by membrane depolarisation, and Ca^{2+} release from inositol-1,4,5-trisphosphate (IP_3) and ryanodine-sensitive intracellular Ca^{2+} stores are the major contributors to increased $[Ca^{2+}]_i$ (Nelson *et al.*, 1990). Membrane hyperpolarisation, caused by the activation of K^+ channels leading to the closure of L-VDCCs, and Ca^{2+} removal from the cytoplasm due to the activity of sarcoplasmic/endoplasmic reticulum Ca^{2+}-ATPase (SERCA) and plasmalemmal Ca^{2+}-ATPase represent the main factors responsible for vessel relaxation. Both large conductance Ca^{2+} (BK_{Ca}) and voltage-gated (K_V) K^+ channels could be activated under these conditions, thereby hyperpolarising the cell membrane (Nelson & Quayle, 1995).

A selective inhibitor of BK_{Ca} channels, iberiotoxin (IbTX), caused contraction of human saphenous arteries (Milesi *et al.*,

*Author for correspondence; E-mail: S.V.Smirnov@bath.ac.uk
[2]Current address: University Laboratory of Physiology, University of Oxford, Parks Road, Oxford OX1 3PT, U.K.
[3]Current address: Department of Pharmacology and Therapeutics, University of British Columbia, 2176 Health Sciences Mall, Vancouver, BC, Canada V6T 1Z3
Advance online publication: 23 August 2004

1999), and an increase in $[Ca^{2+}]_i$ and vasoconstriction of cerebral arteries from adult but not neonatal rats (Gollasch *et al*., 1998). IbTX also inhibited vasodilatation to nitric oxide and its donors in human coronary artery preconstricted with serotonin (Bychkov *et al*., 1998). Additionally, IbTX potentiated phenylephrine- (PE) induced contraction in rat small mesenteric arteries (Dora *et al*., 2000) and increased noradrenaline-dependent contraction and $[Ca^{2+}]_i$ in fetal and adult arteries of the sheep (Long *et al*., 2000) and hamster cremasteric arterioles (Jackson & Blair, 1998). Charybdotoxin (ChTX), another potent inhibitor of BK_{Ca} channels, contracted blood vessels isolated from rat mesenteric, femoral and carotid arteries (Asano & Nomura, 2002). An important role of BK_{Ca} channels in cerebral vascular reactivity was further supported by experiments with mice lacking the $BK_{Ca}\beta$ subunit, showing reduced BK_{Ca} activity associated with elevated blood pressure and reduced sensitivity of arteries to IbTX (Brenner *et al*., 2000; Plüger *et al*., 2000). These findings lead to the conclusion that a transient Ca^{2+} release from the ryanodine-sensitive Ca^{2+} stores (Ca^{2+} sparks) causes a local increase in $[Ca^{2+}]_i$ sufficient to activate BK_{Ca} and may therefore represent a common mechanism by which the BK_{Ca} channels contribute to the regulation of basal vascular tone (Jaggar *et al*., 1998).

The role of K_V channels in pulmonary circulation is well documented (Coppock *et al*., 2001). Also, it has been previously demonstrated that application of nonselective inhibitors of K_V channels such as 4-aminopyridine (4-AP) or 3,4-diaminopyridine caused or augmented agonist- and KCl-induced contractions of arteries and arterioles from various vascular beds of different animal species (Uchida *et al*., 1986; Knot & Nelson, 1995; Doi *et al*., 2000; Shimizu *et al*., 2000; Cheong *et al*., 2001b; 2002), including humans (Uchida *et al*., 1986). In rabbit coronary and middle cerebral arteries, the effect of aminopyridines was mimicked by IbTX or ChTX and low ($\leqslant 1$ mM) concentrations of TEA (Knot & Nelson, 1995; Shimizu *et al*., 2000), suggesting that K_V channels act in concert with BK_{Ca} to regulate vascular tone in some blood vessels. However, in rabbit cerebral arterioles preconstricted with endothelin-1, penitrem A (another specific BK_{Ca} channel inhibitor) had no effect on vascular tone (Cheong *et al*., 2002). In this study, patch-clamp observations of K^+ currents in single myocytes (recorded under conditions when pipette Ca^{2+} buffering was minimised) showed that K_V currents appeared at more negative voltages than BK_{Ca} (Cheong *et al*., 2002), suggesting a greater contribution of the K_V (compared to the BK_{Ca}) channels in the control of the resting membrane potential in small blood vessels.

The rat aorta is widely used as an experimental model to study various aspects of electro- and pharmacomechanical coupling in physiological and pathophysiological states (Shimamura *et al*., 1999). However, very little is known about the relative contribution of the K_V channel currents (I_{K_v}), compared to BK_{Ca} currents, in the control of smooth muscle excitability in this artery. It is also unknown whether an augmentation of $[Ca^{2+}]_i$, which occurs in the presence of vasoconstrictors would alter the I_{K_v} properties in this tissue, for example, by inhibiting the current favouring membrane depolarisation as proposed in Gelband & Hume (1995). Therefore, we investigated the functional role and properties of the whole-cell I_{K_v} in single RAMs dialysed with an elevated free Ca^{2+} (200 and 444 nM) pipette solution to mimic an increased $[Ca^{2+}]_i$ in stimulated arteries (Chen & Rembold, 1995; Aalkjær *et al*., 1998; Knot & Nelson, 1998) including aortas (Bruschi *et al*., 1988; Bova *et al*., 1990; Papageorgiou & Morgan, 1991), and compared these with whole-cell BK_{Ca} current characteristics. The pharmacological profile of the I_{K_v} and the BK_{Ca} current was then used to assess the relative contribution of each conductance to both resting tone and PE-induced contraction in endothelium-denuded aortic preparations. Our findings suggest that I_{K_v} (which is likely to be mediated by K^+ efflux predominantly *via* $K_V2.1$ channels), and not the BK_{Ca} current, is the main K^+ conductance activated in both resting and stimulated aortic SMCs. In addition, an increased $[Ca^{2+}]_i$ altered the voltage-dependent characteristics or the I_{K_v} resulting in the augmentation of the current in the physiological range of membrane potentials.

Methods

Male Wistar rats (weight 225–300 g) were killed by cervical dislocation in accordance with U.K. Home Office guidelines, and the midpart of the thoracic aorta was removed, cleaned of connective tissue and cut into rings, which were then either used for enzymatic cell isolation or tension measurements.

Cell isolation for electrophysiology

Aortic rings (width $\sim$1–1.5 mm) bathed in normal physiological salt solution (PSS) were left on ice for 30 min followed by an incubation in Ca^{2+}-free PSS for 10 min at 37°C. Tissue was then transferred into prewarmed nominally Ca^{2+}-free PSS (3 ml) containing 1 mg ml^{-1} collagenase (Type XI) and incubated for 10 min at 37°C. After gentle trituration, pieces of tissue were placed in a fresh Ca^{2+}-free PSS with 1 mg ml^{-1} of papain and 1 mM dithiothreitol and incubated for another 10 min at 37°C. The tissue pieces were triturated in enzyme- and Ca^{2+}-free PSS and the papain treatment was repeated two more times. The resulting three volumes of Ca^{2+}-free PSS containing dispersed cells were combined, filtered through 95 μm nylon mesh and centrifuged ($1100 \times g$) for 5 min. The pellet was initially resuspended in 0.5 ml of Ca^{2+}-free PSS and then adjusted to a final volume of 1.5 ml with normal PSS. Cells were stored at $+4$°C and used on the same day.

Composition of solutions and materials

Composition of PSS was (in mM): 130 NaCl, 5 KCl, 1.5 $CaCl_2$, 1.2 $MgCl_2$, 10 HEPES and 10 glucose; pH was adjusted to 7.2 with NaOH. Nominally Ca^{2+}-free PSS had the same composition as PSS, but $CaCl_2$ was omitted. The pipette solution containing 200 nM free $[Ca^{2+}]$ (Maxchelator, Stanford University, U.S.A.) had the following composition (in mM): 110 KCl, 10 NaCl, 5 $MgCl_2$, 10 HEPES, 10 EGTA and 5 mM $CaCl_2$; pH was adjusted to 7.2 with KOH. Calculated 8 or 444 nM free $[Ca^{2+}]$ in the pipette solution was achieved by adding 0.5 or 7 mM instead of 5 mM $CaCl_2$, respectively. Also, the 8 nM Ca^{2+}-containing pipette solution included 5 mM MgATP (Belevych *et al*., 2002; Smirnov *et al*., 2002) and the 444 nM solution had 4 mM $MgCl_2$ instead of 5 mM $MgCl_2$. The pipette solution for perforated patch (PP) recordings contained (in mM): 110 KCl, 10 NaCl, 10 HEPES, 10 EGTA, 0.5 mM $CaCl_2$ and 100 μg ml^{-1} amphotericin B (Sigma, U.K.). The composition of Krebs solution used for tension measurements

was (in mM): 118 NaCl, 25 $NaHCO_3$, 4.9 KCl, 1.2 KH_2SO_4, 2.5 $CaCl_2$, 1.2 $MgSO_4$, 11.7 glucose. 10 mM K^+-containing Krebs was made by equimolar replacement of 4.1 mM NaCl with KCl. Appropriate volumes of TEA (2 M stock) or 4-AP (0.5 M stock solution, pH adjusted to 7.4) were added directly to the organ bath to achieve a required final concentration of the drug.

Basic chemicals were purchased from BDH Merck (U.K.) or Fisher (U.K.). Enzymes for cell isolation, PE, ryanodine, cyclopiazonic acid (CPA) and K^+ channel inhibitors, except IbTX (Latoxan), were purchased from Sigma (U.K.). Correolide was obtained as a gift from Merck (U.S.A.).

Electrophysiological experiments

Cells were placed in a chamber with a volume of 100–200 μl and were continually superfused ($\sim$1 ml min^{-1}) with PSS or the test solution *via* a 5-barrel pipette. Whole-cell membrane currents were recorded using the standard patch-clamp technique at room temperature as described previously (Belevych *et al*., 2002; Smirnov *et al*., 2002). Briefly, currents were recorded using an Axopatch-200B amplifier, Digidata 1200 A/D interface and pCLAMP 8.02 software (Axon Instruments, CA, U.S.A.) at a sample rate of 10 kHz and filtered at 2 kHz. The pipette resistance was 2–5 MΩ when filled with the standard pipette solution. Capacitance transients elicited by a 10 mV hyperpolarising step (filtered at 50 kHz and sampled at 200 kHz) were routinely measured after rupture of the cell membrane. The area under the capacitance transient was used to calculate cell membrane capacitance (C_m). To allow for equilibration of the pipette solution with the cell interior, all recordings were started 5 min after establishing the whole-cell configuration. To analyse adequately changes in key characteristics of K^+ currents (such as activation and inactivation) under variety of experimental conditions, whole-cell currents were measured between -100 and $+80$ or $+100$ mV using either a voltage step or ramp membrane depolarisation, respectively. Holding potential was maintained at -80 mV in all experiments.

Isometric tension recordings

Isolated aortic rings ($\sim$2–2.5 mm width) were mounted at 37°C in an organ bath under 1 g resting tension and equilibrated for 60 min in Krebs solution bubbled with 95% O_2/5% CO_2. Tissue was stimulated with three consecutive applications of 2.5 μM PE followed by washing with Krebs solution before the start of an experimental protocol. Tension was measured using a Biegestab K30 isometric force transducer (Hugo Sack Elektronics, Germany), MacLab/4 s recording unit and Chart v3.6/s software (ADI Instruments, U.K.), and expressed in grams of tension. Data were sampled at 40 Hz. Endothelium was removed by gentle rubbing of the vessel lumen with horse hair and successful removal was verified by the absence of relaxation to 10 μM acetylcholine in arteries precontracted with 2.5 μM PE. Each experimental protocol was repeated in preparations from at least three animals.

Immunocytochemistry

A drop of cell suspension was placed on a glass coverslip and left for 30 min to allow cells to attach to the glass surface. Cells were then fixed with 4% paraformaldehyde and incubated with anti-K_v antibodies (Alomone, Israel) for 3 h. The binding of the primary antibody was detected using goat anti-rabbit IgG secondary antibodies labelled with Alexa Fluor 488 (Molecular Probes) (1 : 500) and examined under a confocal microscope (FV500, v.3.2, Olympus, U.K.). Negative controls were routinely performed in the absence of primary antibodies and showed no significant nonspecific staining under these conditions.

Curve fitting, statistical analysis and data presentation

Electrophysiological data analysis and curve fitting were performed using pCLAMP 8.2 and Origin 6.02 (Microcal Software, Northampton, MA, U.S.A.) software. The results are expressed as mean $\pm$ s.e.m. Data were analysed by Student's unpaired *t*-test and $P<0.05$ was considered to be statistically significant unless otherwise stated.

Results

Effect of BK_{Ca} channel inhibitors on whole-cell K^+ currents

To evaluate the relative contribution of I_{K_v} and BK_{Ca} to the net outward current in the presence of 200 nM $[Ca^{2+}]_i$, the effect of specific BK_{Ca} channel inhibitors, IbTX and paxilline, and the nonselective inhibitor TEA, which blocks BK_{Ca} at concentrations below 1 mM, were studied. Whole-cell currents were recorded in response to a 2 s voltage ramp from -100 to $+100$ mV applied every 10 s. K^+ channel inhibitors were applied cumulatively for 150–200 s, sufficient to allow a new steady-state level to be reached in the presence of each concentration of the blocker. IbTX at concentrations between 1 and 100 nM progressively suppressed the whole-cell current (Figure 1a). It is worth noting that, in the concentration range between 100 and 300 nM, the effect of IbTX saturated and no significant block was further developed (Figure 1a). The mean IC_{50} for IbTX, calculated as described in the legend to Figure 1, was 12 ± 5 nM ($n=5$, Figure 1d). Paxilline, another potent inhibitor of BK_{Ca} currents (Li & Cheung, 1999), suppressed the whole-cell current in a similar manner reaching a saturation level between 0.5 and 1 μM (Figure 1b). The overall potency of paxilline was $\sim$8 times less than that of IbTX (mean $IC_{50}=97\pm19$ nM, $n=7$, $P<0.006$, Figure 1d). TEA blocked the current with a mean $IC_{50}=273\pm37$ μM ($n=6$, Figure 1c and d), which is similar to the values reported for BK_{Ca} channels elsewhere (Langton *et al*., 1991; Khan *et al*., 1997). The residual whole-cell K^+ current was not blocked by the highest concentration of IbTX and paxilline (16 ± 6 and 11 ± 3% of the net current, respectively, $P>0.4$, Figure 1a and b), suggesting that both drugs selectively inhibit the BK_{Ca} current. Therefore, to eliminate the BK_{Ca} component, 1 μM paxilline was used in all subsequent experiments. Based on pharmacological evidence we considered the fraction of the whole-cell current, which was blocked by 1 μM paxilline, as the BK_{Ca} current, while the paxilline-resistant component was assumed to be the I_{K_v}.

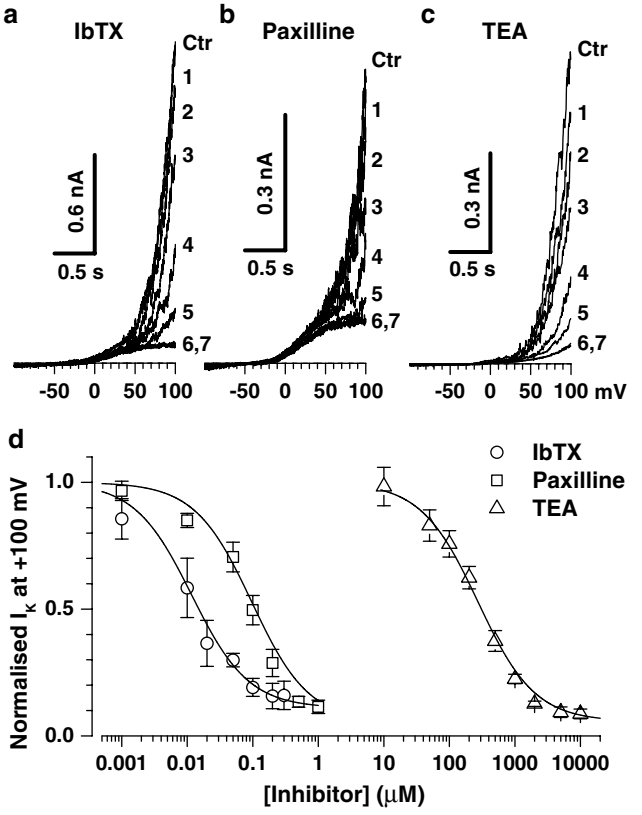

Figure 1 Effect of K^+ channel inhibitors on whole-cell K^+ currents in single rat aortic SMCs. (a–c) Show representative current traces recorded in the presence of various concentrations of IbTX (a), paxilline (b) and TEA (c), added cumulatively. Traces marked from 1 to 7 indicate currents recorded in the presence of 1, 10, 50, 100, 200, 500 and 1000 nM for paxilline (a), 1, 10, 20, 50, 100, 200 and 300 nM for IbTX (b), and 0.01, 0.2, 0.5, 1, 2, 5 and 10 mM for TEA (c), respectively. Ctr indicates control current recording in the absence of the inhibitor. C_m were equal to 10.6 (a), 14.2 (b) and 7.2 (c) pF. (d) Concentration dependence of the inhibition of K^+ current measured at +100 mV by IbTX ($n=5$), paxilline ($n=7$) and TEA ($n=6$). Current traces were recorded with the ramp protocol in the presence of each concentration of the drug (mean of 3–4 traces) and normalised (I_{NORM}) to that in the absence of the drug (mean of 5–10 traces). Solid lines were drawn according to the following equation:

$$I_{NORM} = \frac{1-A}{1+([Drug]/IC_{50})} + A,$$

with a mean IC_{50} of 97 and 12 nM and 273 μM and a residual $A=0.06$, 0.12 and 0.06 for paxilline, IbTX and TEA, respectively, described in the text.

Comparison of the K_V and BK_{Ca} currents in elevated $[Ca^{2+}]_i$

I_{K_v} and BK_{Ca} were compared under three different conditions: cell dialysis with high free $[Ca^{2+}]$ of 200 and 444 nM in the pipette solution and by using PP recordings. This range of Ca^{2+} concentrations is similar to the previously measured global changes in $[Ca^{2+}]_i$ in nonstimulated (~150–200 nM) and stimulated intact aortic preparations and single myocytes (Bruschi *et al*., 1988; Bova *et al*., 1990; Papageorgiou & Morgan, 1991; England *et al*., 1993), thus allowing changes in properties of K^+ currents to be analysed under conditions that mimic a stimulated RAM. Comparison of the whole-cell

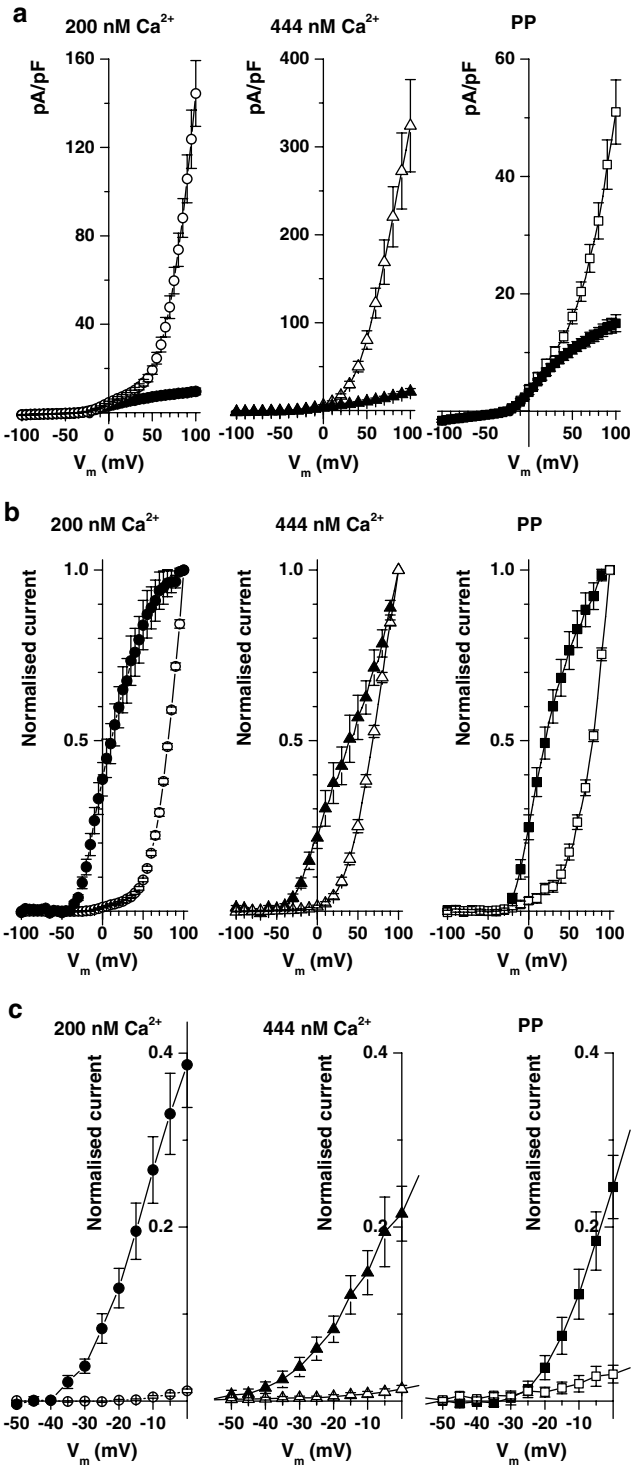

Figure 2 Comparison of K_V and BK_{Ca} currents in RAMs dialysed with different $[Ca^{2+}]_i$ and recorded using the perforated patch mode (as indicated at the top of each panel). (a) Whole-cell currents measured before (open symbols) and after addition of 1 μM paxilline (filled symbols). (b) Comparison of the paxilline sensitive (BK_{Ca}, open circles) and paxilline insensitive (K_V, filled circles) currents. Currents were corrected for a residual leak calculated from the slope resistance measured in the linear range of the I–V (between −100 and −60 mV) in each cell and then normalised to that at +100 mV for each component. (c) Shows the same normalised currents as in (b) but at an expanded scale. Data presented as mean ± s.e.m. for 15 (200 nM), 13 (444 nM) and 19 (perforated patch) RAMs.

currents in cells dialysed with 200 and 444 nM $[Ca^{2+}]_i$ showed that the current was increased to a greater extent at positive potentials (by 200–300% between +30 and +100 mV) than in the negative voltage range (by 15–50% between −30 and 0 mV) (Figure 2a). The BK_{Ca} channel inhibitor paxilline also reduced the current more potently at positive than at negative potentials in the same cell; however, the relative degree of the block was similar in both 200 and 444 nM $[Ca^{2+}]_i$. For example, at +100 mV paxilline blocked 92.7±1.3 and 90.8±1.9% of the whole-cell current, whereas only 35.4±4.7 and 41.2±3.4% of the current was inhibited by the drug at 0 mV in 200 ($n=15$) and 444 ($n=13$) nM $[Ca^{2+}]_i$, respectively. No evidence for a discernible activation of Ca^{2+}-dependent chloride or nonselective conductances was found, since the slope resistance measured in the linear range (between −90 and −60 mV) of the current–voltage (I–V) relationship was not significantly different in cells dialysed with 200 nM (7.9±1.1 GΩ, $n=15$) and 444 nM (10.6±1.8 GΩ, $n=13$) free Ca^{2+}.

To compare the effect of paxilline on the whole-cell current in RAMs in which $[Ca^{2+}]_i$ was not influenced by the pipette Ca^{2+} buffer, PP recordings were performed (Figure 2a, right panel). As can be seen from the figure, a significant component of the paxilline-insensitive current was present over a wide range of membrane potentials, suggesting that the activation of the BK_{Ca} current is relatively small under resting conditions.

To analyse the relative contribution of the BK_{Ca} and I_{K_v} recorded in two pipette $[Ca^{2+}]$ and in the perforated patch mode, the *I–V*'s of the paxilline-sensitive and -insensitive currents were leak corrected, normalised to the current at +100 mV and compared over the whole range of membrane potential tested (Figure 2b), and also at the expanded scale in Figure 2c. This comparison clearly shows that the paxilline-insensitive K_V channel current was activated at more negative potentials than the paxilline-sensitive BK_{Ca} current under all three experimental conditions. These results strongly suggest that, despite the increased $[Ca^{2+}]_i$, the I_{K_v} is the predominant K^+ current activated close to the resting membrane potential measured in rat aortic smooth muscle preparations (Chen & Suzuki, 1989).

Steady-state activation and availability of I_{K_v} *in elevated* $[Ca^{2+}]_i$

It has been previously suggested that elevation of intracellular Ca^{2+} concentration can inhibit I_{K_v} in VSMCs (Gelband & Hume, 1995). We therefore compared the maximal conductance for the I_{K_v} measured under the three experimental conditions described above. Since the current amplitude is significantly underestimated when measured with the ramp protocol (data not shown), *I–V* relationships for the peak I_{K_v} were derived from currents measured using a 300 ms test pulse applied between −100 and +80 mV. The peak amplitude of the I_{K_v} was derived as an asymptotic value of a single exponential fit of the current activation kinetic (as previously described Belevych *et al*., 2002; Smirnov *et al*., 2002). The peak I_{K_v} was converted into conductance assuming the K^+ equilibrium potential to be equal to −83 mV, plotted against membrane voltage and fitted with the standard Boltzmann function in order to attain the maximal conductance (G_{max}), the half-activation (V_a) and the slope factor (k_a) values. Figure 3a compares the averaged conductance–voltage relationships obtained in 200 and 444 nM $[Ca^{2+}]_i$ and in the PP mode. The mean G_{max} was similar for I_{K_v} measured in 444 nM $[Ca^{2+}]$ (87±12 pS/pF, $n=15$) and with the PP technique 86±8 pS/pF, $n=9$). Although G_{max} was increased in 200 nM $[Ca^{2+}]$ (114±20 pS/pF, $n=15$), this value was not significant compared to the other two conditions. Interestingly, no significant differences in V_a and k_a values were found in 200 nM $[Ca^{2+}]_i$ (−4.9±2 and 14.7±0.7 mV, respectively, $n=15$) compared to those obtained with PP recordings (−4.7±4.1 and 14.1±1.4 mV, respectively, $n=9$). However, cell dialysis with $[Ca^{2+}]_i=444$ nM shifted the steady-state

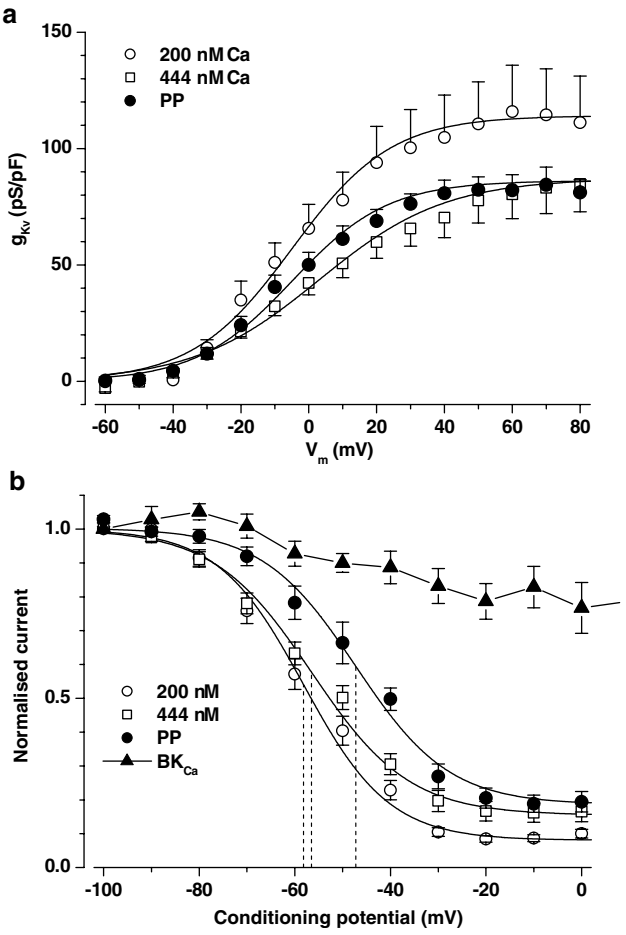

Figure 3 Comparison of the voltage-dependent characteristics of the I_{K_v} recorded in different $[Ca^{2+}]_i$. (a) Steady-state activation of the I_{K_v} measured with 300 ms step protocol. Currents in each cell were leak subtracted, converted into conductance densities (g_{K_v}), averaged and plotted against membrane potential (V_m). g_{K_v} measured in 15, 15 and 9 RAMs using 200 and 444 nM pipette Ca^{2+} and PP, respectively, were averaged and fitted with the standard Boltzmann function (solid lines) with the mean parameters described in the text. (b) I_{K_v} availabilities measured at the test potential +60 mV followed 10 s conditioning membrane depolarisations between −100 and 0 mV. The interval between two pulses was 10 ms. Current amplitude measured during the test step was normalised to the maximal current recorded at a conditioning potential of −90 or −100 mV. The averaged normalised I_{K_v} was then fitted to the Boltzmann function with inactivation parameters described in the text. Dashed lines indicate half-inactivation potentials. Solid triangles show availability of the BK_{Ca} current measured at the test potential of +100 mV in the absence of paxilline ($n=6$). All experiments were performed in the presence of 1 μM paxilline unless otherwise indicated. Holding potential −80 mV.

activation dependency to the right by ~8 mV ($V_a = 3 \pm 2.1$ mV, $P < 0.011$ when compared with 200 nM Ca^{2+} and $P < 0.037$ when compared with the PP using one-tailed *t*-test). Also, the k_a value (which represents the maximum exponential slope of the activation curve) was significantly increased to 18.6 ± 1.1 mV ($n = 15$, $0.007 < P < 0.023$).

The effect of $[Ca^{2+}]_i$ on the I_{K_v} inactivation was assessed using a two-step voltage protocol as described in the legend to Figure 3b. The standard Boltzmann equation was used to compare statistically the effect of increased $[Ca^{2+}]_i$ on the availability of I_{K_v} in RAMs. The I_{K_v} inactivation dependence was shifted by ~10 mV to more negative membrane voltages in RAMs dialysed with 200 nM free Ca^{2+} (the half-inactivation potential, V_h, was -58.2 ± 2.1 mV, $n = 15$) or 444 nM free Ca^{2+} ($V_h = -56.5 \pm 1.9$ mV, $n = 15$) in comparison to nondialysed cells ($V_h = -47.2 \pm 3.3$ mV, $n = 6$, $0.008 < P < 0.012$). In elevated $[Ca^{2+}]_i$, a small but significant increase in the slope factor, k_h, (10.22 ± 0.41 mV, $n = 15$) and in the noninactivating component (0.15 ± 0.03, $n = 15$) was observed in comparison to those obtained with the 200 nM Ca^{2+} in the pipette solution (8.96 ± 0.38 and 0.08 ± 0.01 mV, respectively, $n = 15$, $0.01 < P < 0.022$). In perforated patch recordings, although no significant change in the mean k_h was found (9.77 ± 1.34 mV, $n = 6$) compared to dialysed RAMs, the I_{K_v} inactivated to a significantly smaller degree (0.19 ± 0.02, $P < 0.0001$) than that in 200 nM Ca^{2+}.

It is worth noting that the BK_{Ca} was not significantly inactivated in this range of membrane potentials (Figure 3b). Thus, when the two-pulse voltage protocol was applied in the absence of paxilline, the overall suppression of the current amplitude measured at the test pulse to +100 mV (mainly the BK_{Ca}) by conditioning depolarisation between −40 and 0 mV was only 11–23%.

Pharmacological characterisation of I_{K_v} and immunocytochemical detection of K_V α-isoforms

Expression of multiple types of K_V1 α-genes has previously been detected in rat aorta (Cox *et al*., 2001). We have also shown protein expression of $K_V1.2$, $K_V1.5$ and $K_V2.1$ α-subunits in adult rat aortic smooth muscle (Belevych *et al*., 2002). To verify whether members of the Kv1 subfamily contribute to the I_{K_v} in RAMs, 1 μM correolide, a nortriterpene purified from the tree *Spachea correae* that blocks all K_V1 channels in the nM range (Felix *et al*., 1999; Hanner *et al*., 1999), was used. Cells were stimulated every 10 s with a 300 ms voltage step to +60 mV and correolide was applied at time point 0. No significant inhibition of the current was observed in six RAMs studied (Figure 4a (left) and b (open circles)). In contrast, in rat conduit pulmonary arterial K_V1 cells (which were used as a positive control since the $I_{K_{v1}}$ is thought to be mediated predominantly by K_V1 α-subunits (Smirnov *et al*., 2002)), the current was blocked by $61 \pm 5\%$ within the same period of time ($n = 3$, Figure 4a (right panel) and b (filled circles)).

The lack of effect of the selective K_V1 α-subunit inhibitor correolide on I_{K_v} in RAMs suggests that I_{K_v} is likely to be mediated by either the Kv2.1 or the Kv3.1 delayed rectifier channels previously found in vascular SMCs (Coppock *et al*., 2001). One of the most distinguished pharmacological features of both channels is an approximate 30 times difference in their sensitivity to TEA; the $K_V2.1$ is blocked by millimolar, concentrations, while the $K_V3.1b$ by 100 μM concentrations

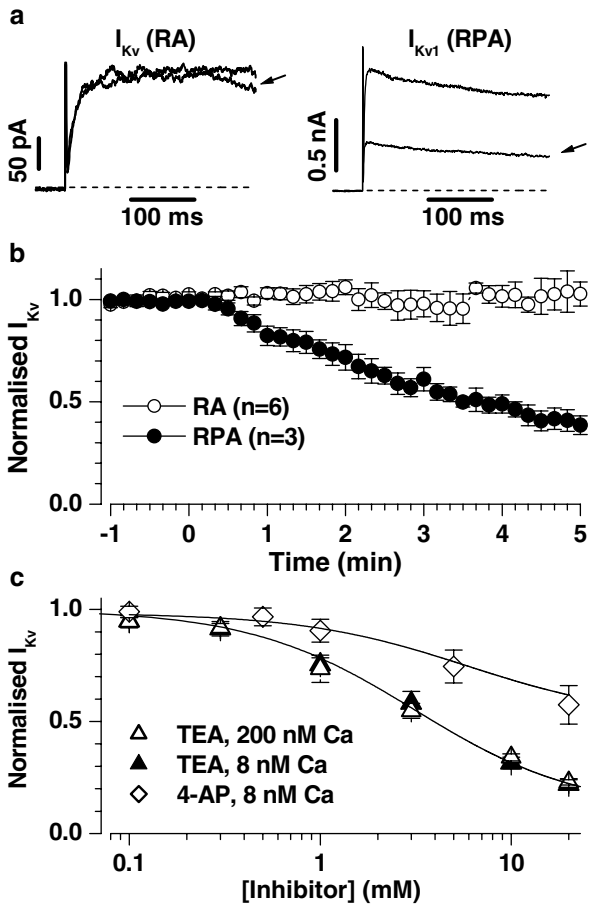

Figure 4 Pharmacological characterisation of I_{K_v}. (a) Effect of 1 μM correolide on I_{K_v} recorded in representative RA cells (left, $C_m = 13.5$ pF) and I_{K1} cell from rat conduit pulmonary artery (RPA, right, $C_m = 6.6$ pF) in the absence and 5 min after application of the inhibitor (shown by arrows). (b) Time dependence of the effect of correolide (applied at time 0) on the I_{K_v} in six RAMs and three RPA cells ($P > 0.22$, paired *t*-test). Current was normalised to the mean current recorded in the absence of the inhibitor. RPA cells were isolated and $I_{K_{v1}}$ current was defined in a manner previously described in (Smirnov *et al*., 2002). (c) Effect of TEA and 4-AP on I_{K_v}. Cells were dialysed with either 200 nM ($n = 5$) or 8 nM (TEA, $n = 3$, 4-AP, $n = 7$) free Ca^{2+} and I_{K_v} was measured with a 300 ms step to +60 mV applied every 10 s. Inhibitors were added cumulatively and the current amplitude, in the presence of each concentration of the drug, was normalised to that in the absence of TEA. Solid lines were drawn according to the equation described in the legend to Figure 1 with the mean IC_{50} and *A* values described in the text.

of TEA (Post *et al*., 1996). Therefore, the TEA sensitivity of the I_{K_v} recorded using the same protocol as for correolide was investigated in RAMs dialysed with 200 nM Ca^{2+}. Cumulative addition of TEA blocked I_{K_v} in a concentration-dependent manner with a mean IC_{50} of 3.1 ± 0.6 mM and a residual component $A = 0.1 \pm 0.02$ ($n = 5$, Figure 4c). A similar effect of TEA ($IC_{50} = 3.2 \pm 0.7$ mM, $A = 0.1 \pm 0.01$, $n = 3$) was also observed under conditions when the pipette solution contained 8 nM free Ca^{2+} in the presence of both 1 μM paxilline and 10 μM glibenclamide in the external PSS (Figure 4c). Cumulative addition of 4-AP also blocked the I_{K_v} (recorded with high buffered pipette Ca^{2+}) in the millimolar concentration range with a mean $IC_{50} = 5.9 \pm 1.9$ mM and $A = 0.5 \pm 0.08$ ($n = 7$, Figure 4c).

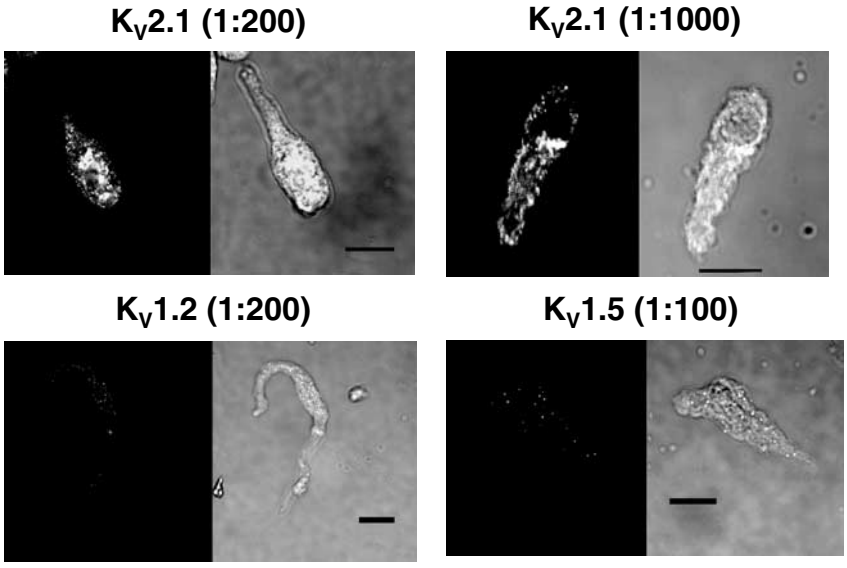

Figure 5 Immunocytochemical detection of K_V channels in RAMs. Localisation of K_V subunits in rat aortic SMCs which were fixed, permeabilised and stained with corresponding anti-K_V2.1, anti-K_V1.2 and anti-K_V1.5 antibodies at dilutions indicated within parentheses. Confocal images and superimposed confocal and transmitted light images are shown on the left and right in each panel, respectively. Horizontal bars 10 μM.

Immunostaining of single rat aortic SMCs with anti-K_V1.2, anti-K_V1.5 and anti-K_V2.1 antibodies clearly demonstrated a strong labelling for the K_V2.1 α-protein using both lower and higher antibody dilutions, while only weak staining was detected for anti-K_V1.2 and anti-K_V1.5 antibodies (Figure 5).

Effect of changes in $[Ca^{2+}]_i$ on the whole-cell steady-state I_{K_v} current in RAMs

Changes in the voltage-dependent characteristics of I_{K_v} caused by increased $[Ca^{2+}]_i$ (Figure 2) can affect the number of channels open in the physiological range of membrane potential (Nelson & Quayle, 1995). To evaluate this possibility, we calculated the steady-state I_{K_v} as a product of activation and inactivation functions, using the mean activation and inactivation parameters described in the text. Figure 6 compares the predicted whole-cell steady-state I_{K_v} (also referred to as the 'window current') calculated for $[Ca^{2+}]_i$ equal to 200 nM (black line) and 444 nM (grey line) and for that in nondialysed RAMs (dashed line). Although the steady-state I_{K_v} was reduced in dialysed cells compared to nondialysed RAMs, the comparison of the 'window' I_{K_v} under controlled $[Ca^{2+}]_i$ showed an approximately two-fold increase in the $[Ca^{2+}]_i$ augmented the steady-state I_{K_v} over the physiological range of membrane potentials. For example, at -60 and -30 mV the whole-cell open state probability of I_{K_v} increased from 0.013 to 0.019 and from 0.006 to 0.01, respectively. Such an increase in I_{K_v} could assist membrane repolarisation and lead to relaxation of the aorta during agonist-induced elevation of $[Ca^{2+}]_i$.

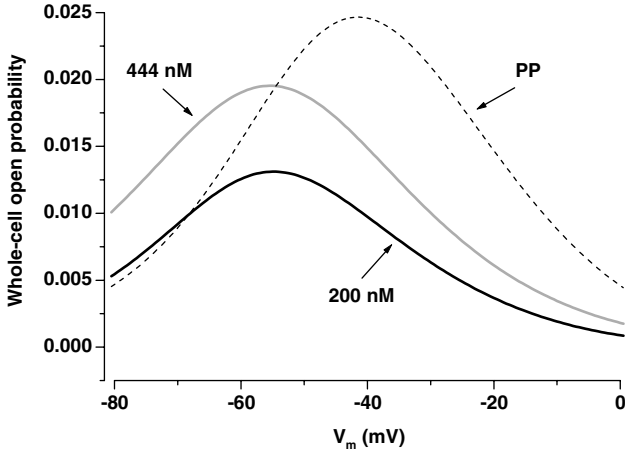

Figure 6 Comparison of the whole-cell steady-state I_{K_v}. The predicted steady-state I_{K_v} (expressed as a fraction of 1) was derived from the product of the steady-state activation and availability dependences with the mean half-activation and half-inactivation potentials and slope factor values recorded in the presence of PP (dotted line), 200 (solid line) and 444 (grey line) nM free Ca^{2+} in the pipette solution as described in the text. The noninactivating component of the current has not been taken into account in this analysis.

Contribution of I_{K_v} to the control of resting tension in rat aorta

To investigate the contribution of K_v currents to the resting tension, the effects of K^+ channel inhibitors were evaluated in the presence of 10 mM K^+ in order to depolarise the cell membrane and enhance the K^+ channel activity. Application of similar concentrations of K^+ produced $\sim$5 mV membrane depolarisation in rat conduit pulmonary arteries (Chen & Suzuki, 1989), but generally did not cause a significant effect on the basal tension (Auer & Ward, 1998; Andersen *et al*., 1999; Doi *et al*., 2000). Under our experimental conditions, no significant difference in the basal tension measured in Krebs and 10 mM K^+ solutions (0.57 ± 0.02 *versus* 0.58 ± 0.02 g, respectively, $n = 30$) was found. Cumulative addition of TEA between 1 and 5 mM induced contractions with superimposed twitch-like oscillations (Figure 7a). An increase in the TEA

concentration up to 10–20 mM caused only a slight further increase in the tonic component. In normal Krebs solution (5.9 mM K^+), contractions to the same concentrations of TEA were observed less frequently than in elevated 10 mM K^+ (Figure 7c). For example, only 3/34 and 5/34 preparations contracted in response to 1 and 5 mM TEA, respectively, in comparison to 3/13 and 8/17 aortic rings maintained in the presence of 10 mM K^+. It is worth noting that responses to low concentrations of TEA were nearly maximal and tended to decrease spontaneously despite the presence of the inhibitor, which made analysis of the TEA concentration-dependent relationship difficult. Therefore, the frequency of occurrence of the TEA-induced response, measured as the presence of contraction and/or oscillations normalised to the total number of experiments performed with each dose of TEA, was measured instead. The frequency response demonstrates that TEA-induced contractions are facilitated by higher doses of the drug and in the presence of 10 mM K^+ (Figure 7c).

Application of 5 and 10 mM 4-AP also induced contractions similar to those induced by TEA (data not shown). 4-AP (5 mM) triggered contraction in 1/5 and 2/4 preparations in the absence and presence of 10 mM K^+ solution, respectively, whereas 10 mM 4-AP constricted all aortic rings tested ($n=6$). A lower dose of 4-AP (1 mM), however, did not cause contraction either in the absence ($n=5$) or in the presence of 10 mM K^+ ($n=4$).

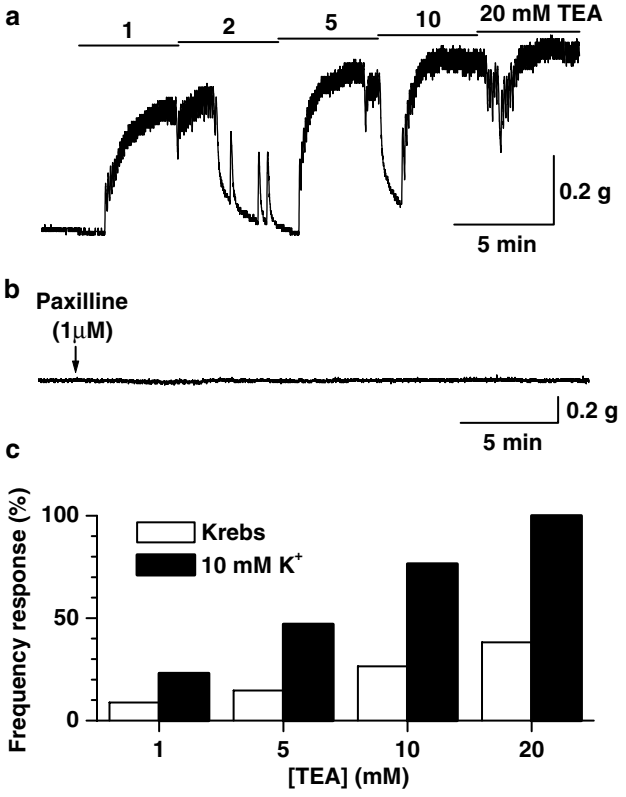

Figure 7 The effect of TEA and paxilline on the basal tone in the endothelium-denuded rat aorta in the presence of 10 mM K^+. (a) Effect of cumulative addition of TEA. (b) Effect of 1 μM paxilline. (c) Comparison of the percentage of preparations eliciting TEA-induced contraction in normal Krebs and 10 mM K^+ solutions. Frequency response was measured as a percentage ratio of contractions evoked by each concentration of TEA to the total number of applications of the inhibitor in normal Krebs solution (open bars, total attempts = 34) and in the presence of 10 mM K^+ (solid bars, total attempts = 17, except 1 mM where $n=13$).

In the presence of 10 mM K^+, the addition of 1 μM paxilline (Figure 7b, $n=7$) or 10 μM glibenclamide ($n=5$), a selective inhibitor of ATP-sensitive K^+ (K_{ATP}) channels, or combination of both drugs ($n=3$) applied for 30 min did not produce a contraction.

Role of I_{K_v} in agonist-induced contraction in rat aorta

To investigate which type of K^+ current was activated in rat aorta stimulated with an agonist, the effects of the K^+ channel inhibitors (TEA, 4-AP, paxilline, IbTX and correolide) were studied on PE-induced contractions. Aortic rings were stimulated with concentrations of PE between 15 and 40 nM, close to the half-maximal response for PE in endothelium-denuded rat aorta ($EC_{50}=31\pm5$ nM, $n=13$, our unpublished observation). Application of submaximal PE concentrations produced a complex response causing an initial increase in the basal tension, followed by superimposed slow waves of contractions (termed oscillatory waves or OWs) (Figures 8 and 9). Each OW was characterised by a marked plateau with superimposed periodic fluctuations probably representing the summation of several shorter twitch-like contractions (Figures 8 and 9, insets). OWs were consistently evoked by low PE concentrations (including two preparations which required 50 and 80 nM) in 65/73 aortic rings obtained from 25 animals. In the remaining eight preparations, four showed only periodical twitch-like contractions and four produced sustained tension with superimposed fluctuations of small amplitude.

Since, as described below, the K^+ channels inhibitors affected only rhythmic activity but not sustained contraction, OWs were characterised quantitatively by measuring the amplitude, as the difference between the maximal and the minimal amplitudes, and the duration at 50% of the maximal amplitude of OWs. Each measurement was calculated as an average of at least three OWs, giving a mean OW duration of 113 ± 5 s ($n=65$, range 21–252 s). Variations in both the amplitude (range 133–720 mg with a mean value of 359 ± 15 mg) and the frequency (range 0.13–1.32 waves/min with a mean of 0.29 ± 0.02 waves/min) of OWs were also observed ($n=65$). The mean sustained tension (measured as the difference between the minimum active tension achieved for a given dose of a drug and the resting tension measured in the absence of any stimulants) developed at these concentrations of PE was 0.34 ± 0.02 g ($n=65$). No correlation between the magnitude of sustained contraction and the amplitude, the frequency or the duration of OWs was found (correlation coefficient was between 0.02 and 0.36).

OWs were suppressed by 0.2–1 μM diltiazem, a selective inhibitor of L-VDCC, and by 1–2 μM ryanodine, which inhibits Ca^{2+} release from ryanodine-sensitive stores, (Figure 8a and b, respectively). Both agents blocked OWs in a similar manner, causing an initial shortening of OWs by decreasing the number of individual twitch-like contractions within OWs, followed by complete cessation of OWs (Figure 8a and b, insets). In addition, OWs were rapidly inhibited by 5–10 μM CPA (a SERCA inhibitor). The effect of CPA was also associated with a gradual increase in the sustained tension (Figure 8c), whereas no significant inhibition of PE-induced sustained contraction was found in the presence of diltiazem or ryanodine (Figure 8a and b). It is worth mentioning that OWs

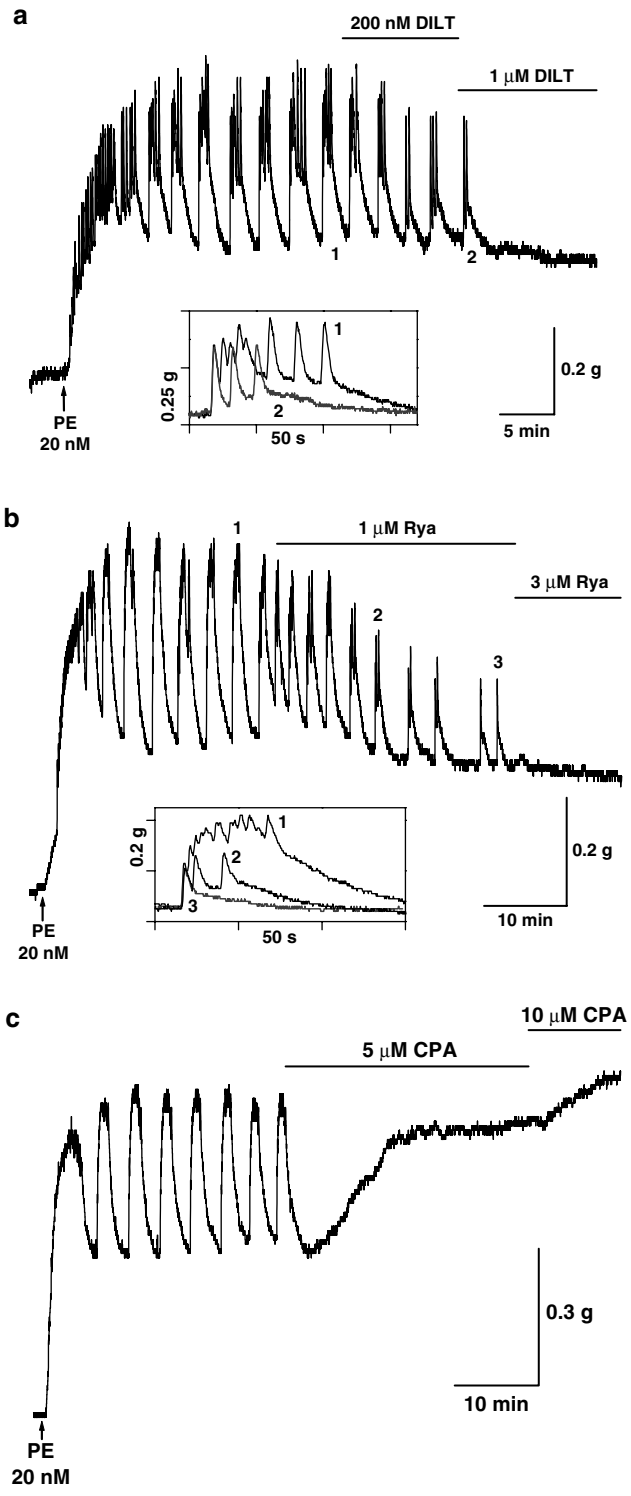

Figure 8 Effect of diltiazem, ryanodine and CPA on PE-induced rhythmic contractions in the endothelium-denuded rat aorta. (a) Effect of 200 nM and 1 μM of diltiazem (DILT). *Inset*: two superimposed OWs before (trace 1) and after addition of 200 nM diltiazem (trace 2). Traces were aligned at the beginning of each OW to aid comparison. (b) Effect of 1 and 3 μM ryanodine (Rya) on PE-induced OWs. *Inset*: superimposed traces before (1) and in the presence of 1 μM ryanodine (2 and 3). The baseline in traces 2 and 3 was adjusted by 10 and 40 mg, respectively, for better alignment with trace 1. Note that neither diltiazem nor ryanodine affected the PE-induced sustained contraction. (c) Effect of 5 and 10 μM CPA. Traces in (a–c) were recorded from three different preparations.

were not blocked by 50 μM niflumic acid, an inhibitor of Ca^{2+}-activated Cl^- channels, suggesting that activation of this conductance was not essential for the generation of rhythmic activity under our experimental conditions (data not shown).

The addition of increasing concentrations of TEA caused a progressive increase in the amplitude and duration of OWs (Figure 9a), as expected from the inhibition of TEA-sensitive K^+ channels participating in the OW relaxation process. Application of 4-AP caused two effects: an initial transient decrease in the PE-induced sustained contraction and a significant increase in both the amplitude and duration of OWs (Figure 9b). Although the reason for the 4-AP-dependent decrease in tension is not clear, we did not observe any relaxant effect of 4-AP on the basal tension measured both in Krebs and 10 mM K^+ solutions, indicating that the development of some tone is required for this to be observed. Nevertheless, the effect of 4-AP on the duration and amplitude of OWs was very similar to that of TEA, suggesting that the K^+ conductance involved in the regulation of rhythmic activity is also 4-AP sensitive. A marked reduction in the frequency of OWs usually observed in the presence of 4-AP could be partially due to a decreased level of sustained contraction in the presence of the drug. For example, the sustained tension was decreased by $8 \pm 2\%$ ($n = 7$) and $12 \pm 2\%$ ($n = 5$) in the presence of 1 and 5 mM 4-AP, respectively. It is worth noting that with time a slow decrease in the PE-induced sustained tension, observed in some preparations, caused a reduction in the frequency of OWs. This was also associated with a decrease in the duration and amplitude of OWs; effects which are opposite to those observed in the presence of 4-AP. In contrast to TEA and 4-AP, addition of the BK_{Ca} channel inhibitors paxilline (Figure 9c) or IbTX (Figure 9d) had no significant effect on the amplitude and duration of OWs, nor the sustained tension, suggesting that BK_{Ca} currents are not involved in the regulation of PE-induced contraction of rat aortic smooth muscle.

To compare quantitatively the effect of K^+ channel inhibitors on OWs in all preparations, relative changes in the amplitude and duration of OWs observed in the presence of K^+ channel inhibitors were averaged expressed as a percentage, and plotted against the corresponding concentration of the drug (Figure 10). The mean changes in both the amplitude and duration of OWs observed in the presence of TEA or 4-AP (both at 5 mM) were significantly different from those measured in the presence of the maximal concentration of the BK_{Ca} channel inhibitors ($0.008 < P < 0.03$). In addition to this, application of 1 μM correolide for at least 30 min did not significantly affect either the amplitude ($1.6 \pm 6.1\%$) or the duration ($-5.9 \pm 9.1\%$) of OWs in six aortic rings tested, suggesting that $K_V\alpha 1$ channels are not active in SMCs in the intact preparation.

Discussion

Our primary findings demonstrate that K_V currents (*via* channels formed mainly by $K_V2.1$ α-subunits), and not BK_{Ca} currents, are responsible not only for maintaining the resting tension of rat aorta but also for the regulation of induced rhythmic activity of this tissue. The characterisation of the I_{K_v} in cells dialysed with 200 and 444 nM free Ca^{2+} demonstrated significant changes in the voltage-dependent properties, but

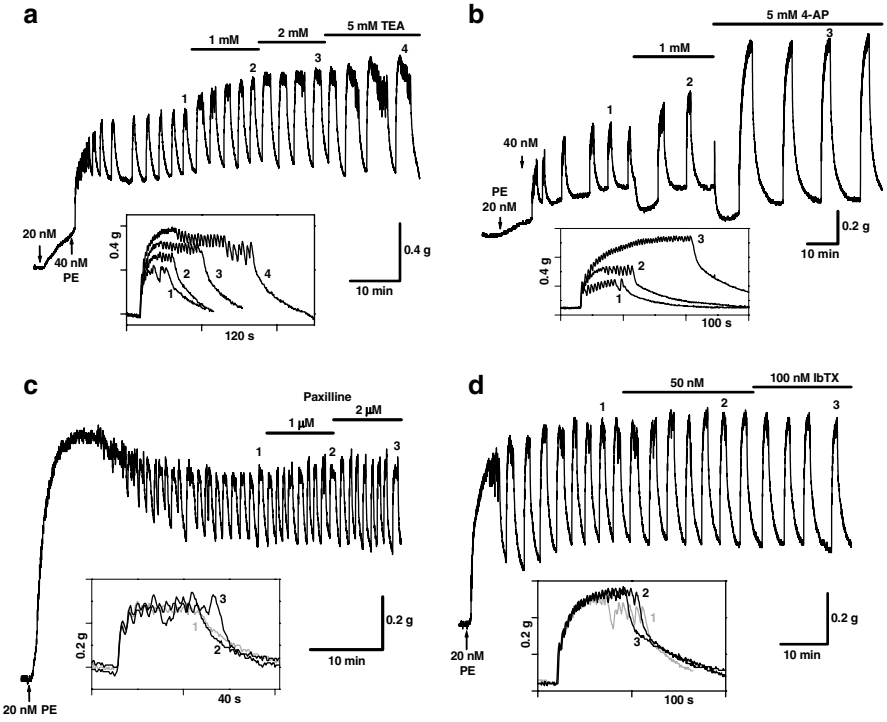

Figure 9 The effect of K^+ channel blockers on PE-induced rhythmic activity in endothelium-denuded rat aorta. (a–d) show the effect of various concentrations of TEA, 4-AP, paxilline and IbTX on OWs, respectively. *Insets*: superimposed OWs marked by letters in the absence and presence of the K^+ channel inhibitors. In order to facilitate a comparison, the baseline was adjusted by 96 (trace 2), 59 (trace 3) and 21 (trace 4) mg in panel (a), by 90 mg (trace 3) in panel (b), and by 19 (trace 2) and 43 (trace 3) mg in panel (d).

not in the maximal conductance, of the K_V current. This can lead to the enhancement of the I_{K_v} in the physiological range of membrane potentials, thereby promoting membrane hyperpolarisation.

I_{K_v} *is the predominant* K^+ *conductance in rat aortic myocytes*

To differentiate between the K_V and BK_{Ca} channel currents, we used 1 μM paxilline in most of our experiments. Despite being several times less potent than IbTX, paxilline selectively blocked BK_{Ca} currents with an $IC_{50} = 97$ nM (Figure 1), which was similar to that reported previously for BK_{Ca} currents in rat mesenteric arterial myocytes ($IC_{50} = 37.5$ nM) (Li & Cheung, 1999). Based on the sensitivity to paxilline, we considered the paxilline-sensitive component of the whole-cell current as BK_{Ca}, while the paxilline-resistant component was assumed to predominantly be the K_V current.

In perforated patch recordings (Figure 2a), the amplitude of the BK_{Ca} current was significantly smaller than that in cells dialysed with 200 or 444 nM $[Ca^{2+}]$, indicating that in nondialysed RAMs $[Ca^{2+}]_i$ is maintained at low levels close to the plasmalemmal membrane. An increase in $[Ca^{2+}]_i$ from 200 to 444 nM (assuming that 5 min was sufficient for equilibration between the pipette solution and the cytosol) resulted in a significant augmentation of the BK_{Ca} current in the positive, and not the negative (<0 mV), voltage range. A comparison of the apparent activation threshold of BK_{Ca} and K_V currents in elevated $[Ca^{2+}]_i$ (Figure 2) clearly demonstrates that the appearance of I_{K_v} was shifted by $\sim$20–30 mV to more negative membrane potentials than that of the BK_{Ca}. These findings echo the results obtained in rabbit cerebral arterioles, where I_{K_v} (recorded with a low Ca^{2+}-buffered pipette solution containing 0.2 mM EGTA) was activated by $\sim$20 mV more negative than BK_{Ca} currents (Cheong *et al*., 2002), and in rat intrapulmonary arterial SMCs, where cell dialysis with $\sim 0.5\,\mu$M $[Ca^{2+}]_i$ only caused a small (16–30%) increase in the amplitude of the TEA-sensitive (BK_{Ca}) current at membrane potentials positive to -10 mV (Smirnov & Aaronson, 1994; Smirnov *et al*., 1994). Furthermore, practically no BK_{Ca} single channel activity was observed below -20 mV in inside–out patches from freshly isolated RAMs or myocytes maintained in primary culture and superfused with 0.1 μM Ca^{2+}, and only a $\sim$10% increase in the channel open probability at -20 mV was observed at 1 μM $[Ca^{2+}]_i$ (Sadoshima *et al*., 1988; England *et al*., 1993). Interestingly, a relatively low Ca^{2+} sensitivity of single BK_{Ca} channels, requiring $>1\,\mu$M Ca^{2+} for the channel to be active at negative voltages, was observed in both rat small cerebral arteries and hamster cremasteric arterioles (Jackson & Blair, 1998), correlating with a low (Liu *et al*., 1998) or complete absence (Jackson & Blair, 1998) of contractile response of intact vessels to IbTX. Conversely, perfusion of single SMCs isolated from human saphenous veins with a pipette solution containing only 0.1 mM EGTA resulted in a marked activation of BK_{Ca} currents in the negative voltage range and application of 50 nM IbTX caused contraction of the intact preparation (Milesi *et al*., 1999). Although the exact reason for the differential Ca^{2+} sensitivity of BK_{Ca} currents in some VSMCs is not clear, possible explanations could include the existence of BK_{Ca} splice variants with a different Ca^{2+} sensitivity (Sansom & Stockand, 1994); differences in the functional

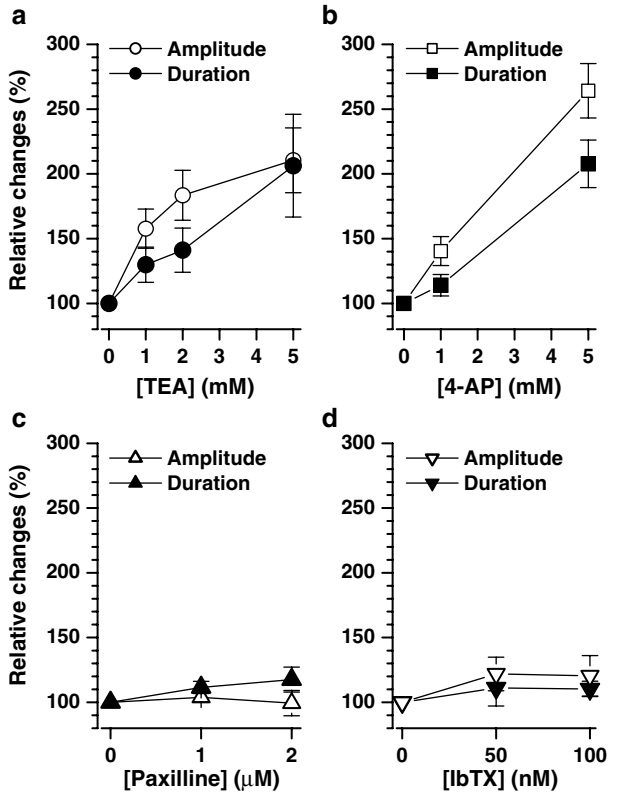

Figure 10 Comparison of the effect of K^+ channel inhibitors. (a–d) summarise the effect of TEA (a), 4-AP (b), paxilline (c) and IbTX (d) on the amplitude and duration of OWs. The amplitude and duration of OWs were measured in the presence of each concentration of a K^+ blocker, normalised to that in the absence of the drug and expressed as percentage of relative change. The control value was measured as the mean of three OWs just before the inhibitor was added to the organ bath and set as 100%. Statistical analysis is given in the text.

expression the BK_{Ca} β-subunits (Brenner *et al*., 2000; Plüger *et al*., 2000) and/or interaction between α and β subunits (Tanaka *et al*., 1997); a spatial distribution of BK_{Ca} channels in VSMCs (e.g. their colocalization with ryanodine receptors allowing a rapid and large increase in $[Ca^{2+}]_i$ in the channel vicinity (Jaggar *et al*., 1998)) or a combination of these and maybe other yet to be identified factors.

Effect of elevated $[Ca^{2+}]_i$ on I_{K_v}

It has been previously suggested that the enhancement of intracellular Ca^{2+} can directly inhibit I_{K_v} in some types of VSMCs (Gelband & Hume, 1995). In rat aortic SMCs, the comparison of conductance–potential relationships of I_{K_v} studied under three different experimental conditions did not reveal significant changes in the maximal conductance of the K_V current (Figure 3a), suggesting that I_{K_v} is not directly blocked by the rise in intracellular Ca^{2+} at least up to $\sim 0.4\,\mu$M in this preparation. Nevertheless, the voltage-dependent characteristics of the I_{K_v} were markedly altered in cells dialysed with increasing $[Ca^{2+}]_i$. The most significant effect was on the I_{K_v} steady-state activation dependence shifting it rightward and decreasing its voltage sensitivity (*via* an increase in the slope factor) by $\sim 30\%$. In addition, a small decrease in the slope of the I_{K_v} availability was also observed at $[Ca^{2+}]_i = 444$ nM. Ca^{2+}-dependent changes in the steady-state voltage-dependent characteristics of the I_{K_v} in RAMs produced an increase in the open state probability of the current (Figure 6) that may be important in membrane hyperpolarisation in agonist-stimulated intact tissue as discussed below. Although differences in the activation and inactivation of the I_{K_v} were observed between dialysed and nondialysed RAMs, a direct comparison of voltage-dependent parameters is complicated by the fact that these characteristics of I_{K_v} in RAMs also depend on the phosphorylation state of the channel (Tammaro *et al*., 2001), as well as on the presence of intracellular magnesium ions (Tammaro & Smirnov, 2003), which may differentially alter the I_{K_v} properties depending on the composition of the pipette solution. This is further supported by a comparison of the I_{K_v} activation and inactivation obtained in the present study with those we previously reported in RAMs dialysed with low $[Ca^{2+}]_i$ (8 nM) and 5 mM MgATP (Belevych *et al*., 2002). Both the activation (mean $V_a = 5.2$ mV) and the availability (mean $V_h = -39.6$ mV) of I_{K_v} was shifted to more positive membrane potentials, which differ from those in RAMs dialysed with 200 nM Ca^{2+} despite the fact that the sensitivity of the I_{K_v} to TEA was virtually the same under both conditions (Figure 4c).

Molecular identity of I_{K_v} in rat aortic SMCs

The molecular identity of delayed rectifier currents in different types of VSMCs is largely unknown, although the gene expression of most K_V isoforms has been demonstrated in various types of blood vessels (Davies & Kozlowski, 2001; Cheong *et al*., 2001b). Recent evidence suggests that, depending on the vessel size and probably animal species, different K_V channel isoforms can be responsible for K_V currents. Thus, in cerebral circulation, $K_V1.2/K_V1.5$ heteromultimers are likely to form I_{K_v} in rat small cerebral arteries (Albarwani *et al*., 2003), whereas different $K_V\alpha1$ isoforms are more important in rabbit ($K_V1.6$ and $K_V1.5$ homo- and/or heteromultimeric complexes; Cheong *et al*., 2001a) and in murine ($K_V1.3$ and $K_V1.6$ homo- and/or hetero-tetramers; Cheong *et al*., 2001b) cerebral arterioles. The members of the $K_V\alpha1$ subfamily ($K_V1.2/K_V1.5$ heteromultimers) together with the $K_V2.1/K_V9.3$ heterotetramers and $K_V3.1b$ homotetramers were also proposed to compose I_{K_v} in pulmonary SMCs (Coppock *et al*., 2001). In rat aorta, the expression of multiple $K_V\alpha1$ and $K_V\alpha2$ genes (Roberds & Tamkun, 1991; Cox *et al*., 2001; Thorne *et al*., 2002) and proteins (Belevych *et al*., 2002; Thorne *et al*., 2002) have been demonstrated previously. However, the analysis of gene and protein expression does not answer the question as to whether the whole-cell I_{K_v} is composed of a single or multiple K_V component in intact RAMs. To address this question, we used a selective $K_V\alpha1$ inhibitor correolide (Felix *et al*., 1999; Hanner *et al*., 1999). Application of 1 μM correolide had no effect on the I_{K_v} in RAMs, despite the significantly suppressed K_V1-mediated current in rat main pulmonary SMCs (Figure 4a and b). These results support our previous findings that I_{K_v} in RAMs was not blocked by 200 nM α-dendrotoxin and 300 nM ChTX (Belevych *et al*., 2002), suggesting that K_V1 α-subunits are unlikely to contribute to the native I_{K_v} in this tissue. The $K_V3.1b$ channel is sensitive to both TEA and 4-AP in the micromolar range (Grissmer *et al*., 1994; Post *et al*., 1996). On the other hand, a relatively slow kinetic of activation of I_{K_v}

and millimolar sensitivity to 4-AP (Belevych *et al*., 2002) and TEA (this paper) are characteristic features of the cloned $K_V2.1$ channels (Post *et al*., 1996), pointing towards the $K_V2.1$ α-subunit as the main component of the K_V channel in rat aortic SMCs. The results of the immunocytochemical analysis of the expression of K_V α-subunits also support this conclusion.

Role of K_V channels in the regulation of contraction of rat aorta

The electrophysiological data in single RAMs suggests that I_{K_v} is activated at more negative membrane potentials than BK_{Ca} currents (Figure 2), and could therefore be one of the major currents in this tissue to control membrane potential at rest. To assess whether K_V channels are also active in the intact nonstimulated aorta at rest (i.e. without the development of contraction), the effect of 1–5 mM TEA and 4-AP (K^+ channel inhibitors which block I_{K_v} in RAMs) was studied. Both inhibitors caused a marked contraction of endothelium-denuded rat aortic rings in normal Krebs. Notably, stimulatory effects of 4-AP and TEA were enhanced in the presence of 10 mM K^+, which depolarises large arteries by ~5 mV (Chen & Suzuki, 1989) without significant effects on the basal tension (Auer & Ward, 1998; Andersen *et al*., 1999; Doi *et al*., 2000). Such a small depolarisation should significantly increase the activation of voltage-dependent K^+ channels, such as K_V and BK_{Ca}, in the negative voltage range (Nelson & Quayle, 1995). However, the specific BK_{Ca} inhibitor paxilline did not mimic the effects of TEA and 4-AP under this condition (Figure 7b), which suggests that BK_{Ca} currents are not active at rest in the intact aorta, thus supporting the electrophysiological data obtained in single cells. The lack of effect by the selective K_{ATP} channel inhibitor glibenclamide also rules out a significant contribution of K_{ATP} currents to the regulation of the basal tone in this tissue. Interestingly, potentiation of agonist- and KCl-induced contraction by mM concentrations of 4-AP and TEA was also observed in mouse (Jiang *et al*., 1999) and rabbit (Cook, 1989) aortas, indicating that activation of a similar type of K^+ conductance might contribute to the control of aortic contractility in other species.

Since activation of BK_{Ca} currents can be significantly increased in the stimulated tissue by local increases in $[Ca^{2+}]_i$ (Pérez *et al*., 2001), the effect of TEA, 4-AP, correolide, paxilline and IbTX on contraction induced by the α_1-adrenoreceptor agonist PE was investigated. The effect of K^+ channel blockers on the KCl-induced contraction has not been studied in detail because a decrease in the K^+ conductance resulting from a reduction in the driving force for potassium ions could make the interpretation of their effects ambiguous, as was demonstrated with the effect of the K^+ channel activator cromakalim on KCl contraction in rat conduit pulmonary arteries (Seiden *et al*., 2000). Application of PE at concentrations close to the EC_{50}-induced slow rhythmic contractions (termed OWs) superimposed on the sustained tension in endothelium-denuded aortic rings. It is worth noting that although shorter twitch-like contractions have been reported in rat aorta (Freeman *et al*., 1995), the type of oscillatory contraction described in this paper has not previously been characterised. Neither IbTX and paxilline (the BK_{Ca} channel inhibitors) nor correolide (which blocks $K_V\alpha1$ channels) caused any significant effect either on the basal tension or OWs. On the other hand, TEA and 4-AP, which blocked I_{K_v} in RAMs, significantly increased both the amplitude and duration of PE-induced OWs, suggesting that TEA- and 4-AP-sensitive I_{K_v} is the predominant K^+ conductance, which operates during α_1-adrenergic stimulation of rat aortic SMCs.

It should be noted that although TEA and 4-AP had a significant effect on PE-induced rhythmic activity, they did not cause an appreciable increase in the sustained tension, suggesting that sustained contraction and OWs could be initiated by different mechanisms. It has been previously shown that stimulation of α_1-adrenoreceptors, in addition to release of Ca^{2+} from IP_3-sensitive stores, also causes membrane depolarisation of VSMCs (Mulvany *et al*., 1982; Chen & Rembold, 1995). Therefore, it is possible that the sustained tension is maintained by IP_3-mediated release from intracellular Ca^{2+} stores, whereas OWs are triggered by membrane depolarisation. The stimulatory effect of the I_{K_v} blockers and the inhibitory effect of the L-VDCC inhibitor diltiazem on OWs, but not on the sustained tension (Figures 8a–10), support the involvement of both types of voltage-dependent ion channels in the initiation of OWs. Additional sensitivity of OWs to ryanodine (Figure 8b), as well as CPA (Figure 8c), indicates the participation of Ca^{2+} release from ryanodine-sensitive Ca^{2+} stores triggered by Ca^{2+} entry *via* L-VDCCs in the generation of OWs. Similar effects of the L-VDCCs inhibitors (such as nifedipine or nicardipine), ryanodine and CPA on endothelium-independent rhythmic contractions were reported in rat pulmonary arteries from animals exposed to chronic hypoxia (Bonnet *et al*., 2001) and treated with monocrotaline (Kiyoshi *et al*., 2003) to induce hypertension. An increase in sustained tension in the presence of CPA is expected, since CPA constricts arteries by releasing Ca^{2+} from both ryanodine- and IP_3-sensitive stores (Shima & Blaustein, 1992; Noguera *et al*., 1998; Tosun *et al*., 1998).

In order to maintain any rhythmic activity, the presence of a negative feedback mechanism is required (Berridge & Galione, 1988; Gustafsson, 1993). If membrane depolarisation is essential to trigger OWs in rat aortic SMCs, then a mechanism capable of hyperpolarising the cell membrane should also be present. In other preparations the BK_{Ca}, activated by the rise of $[Ca^{2+}]_i$ in addition to an increase in the membrane potential, has been proposed to be the main hyperpolarising K^+ conductance. This hypothesis has been supported by the stimulatory effects of IbTX and/or ChTX on rhythmic activity in intact preparations (Gokina *et al*., 1996; Wesselman *et al*., 1997; Jiang *et al*., 1999).

Our experimental evidence entails the involvement of two voltage-dependent conductances in the initiation of rhythmic contraction in rat aorta: L-VDCCs (as the main depolarising conductance) and the delayed rectifier I_{K_v} (as the main hyperpolarising K^+ conductance), which should act as a pure voltage-dependent oscillator coupled to ryanodine-sensitive stores. If this is the case, then changes in the voltage-dependent characteristics of both channel types should be important in providing a negative feedback loop required for oscillatory behaviour. Ca^{2+}-dependent inactivation, a characteristic feature of L-VDCCs in SMCs, can be responsible for the initial reduction of the Ca^{2+} entry *via* L-VDCCs. A subsequent increase in the I_{K_v} activation (as a result of membrane depolarisation caused by L-VDCCs) could progressively hyperpolarise the cell membrane.

Potentiation of the steady-state I_{K_v} at elevated $[Ca^{2+}]_i$ can also contribute to membrane hyperpolarisation in RAMs. In various vascular preparations (Gokina *et al*., 1996; Peng *et al*., 1998; Oishi *et al*., 2002) including rat aortas (Hayashida *et al*., 1986), the amplitude of oscillations in membrane potential ranged between 5 and 20 mV. Although membrane potential was not measured in this study, it is possible to estimate the degree of cell membrane hyperpolarisation caused by an increased $[Ca^{2+}]_i$ using the approach described previously by Nelson and Quayle (1995). Assuming an input resistance of 8 GΩ, which corresponds to a conductance of 125 pS, the total K^+ conductance at −60 mV would be equal to ∼90 pS. The estimated number of K_V channels per a single RAM is equal to 116, assuming the maximal conductance to the equal to 95 pF/pS (Figure 3a), a mean cell capacitance of 12 pF and a single channel conductance of ∼10 pS (Pascual *et al*., 1997; Kramer *et al*., 1998). Taking into account the Ca^{2+}-dependent changes in the open state probability (Figure 6), an increase in the steady-state I_{K_v} conductance at −60 and −30 mV should be equal to 7.5 and 4.3 pS yielding membrane hyperpolarisation of 1.1 and 0.5 mV, respectively, which is comparable to oscillatory changes in membrane potential measured with intracellular microelectrodes (Hayashida *et al*., 1986; Gokina *et al*., 1996; Peng *et al*., 1998; Oishi *et al*., 2002). The Ca_i^{2+}-dependent increase in the steady-state I_{K_v} is unlikely to be due to differences in the pipette Mg^{2+} concentration since a similar effect was also observed in RAMs dialysed with 200 nM compared to 10 nM free Ca^{2+} in the pipette solution containing 0.5 mM $MgCl_2$ (our unpublished observations). Although the precise mechanism of modulation of I_{K_v} by intracellular Ca^{2+} remains unclear and necessitates further experimental evidence, the involvement of Ca^{2+}-dependent protein kinase C (PKC) isoform (e.g. PKCα) in this process is possible (Tammaro *et al*., 2002; Tammaro & Smirnov, 2002).

In conclusion, our findings suggest that the voltage-dependent K^+ current through $K_V2.1$ channels plays a key role in the regulation of contractile activity of rat aorta. Modulation of the voltage-dependent characteristics of I_{K_v} by various intracellular factors including calcium and/or calcium-dependent processes could be important in maintaining the function of K_V channels in the physiological range of membrane potential.

We are grateful to Mr Barry Crowley for technical assistance and Dr G Kaczorowski (Merck, U.S.A.) for the gift of correolide. This work was supported by the British Heart Foundation Grant FS/2000013.

References

AALKJÆR, C., MORTENSEN, F.V., JENSEN, P.E. & NIELSEN, H. (1998). The role of $[Ca^{2+}]_i$, membrane potential and pH_i in the relaxation of rat mesenteric arteries to hyperosmolar acetate. *Pflügers Arch.,* **436,** 705–711.

ALBARWANI, S., NEMETZ, L.T., MADDEN, J.A., TOBIN, A.A., ENGLAND, S.K., PRATT, P.F. & RUSCH, N.J. (2003). Voltage-gated K^+ channels in rat small cerebral arteries: molecular identity of the functional channels. *J. Physiol.,* **551,** 751–763.

ANDERSEN, H.L., WEIS, J.U., FJALLAND, B. & KORSGAARD, N. (1999). Effect of acute and long-term treatment with 17-β-estradiol on the vasomotor responses in the rat aorta. *Br. J. Pharmacol.,* **126,** 159–168.

ASANO, M. & NOMURA, Y. (2002). Contribution of sarcoplasmic reticulum Ca^{2+} to the activation of Ca^{2+}-activated K^+ channels in the resting state of arteries from spontaneously hypertensive rats. *J. Hypertens.,* **20,** 447–454.

AUER, G. & WARD, M.E. (1998). Impaired reactivity of rat aorta to phenylephrine and KCl after prolonged hypoxia: role of the endothelium. *J. Appl. Physiol.,* **85,** 411–417.

BELEVYCH, A.E., BECK, R., TAMMARO, P., POSTON, L. & SMIRNOV, S.V. (2002). Developmental changes in the functional characteristics and expression of voltage-gated K^+ channel currents in rat aortic myocytes. *Cardiovasc. Res.,* **54,** 152–161.

BERRIDGE, M.J. & GALIONE, A. (1988). Cytosolic calcium oscillators. *FASEB J.,* **2,** 3074–3082.

BONNET, S., HYVELIN, J.M., BONNET, P., MARTHAN, R. & SAVINEAU, J.P. (2001). Chronic hypoxia-induced spontaneous and rhythmic contractions in the rat main pulmonary artery. *Am. J. Physiol.,* **281,** L183–L192.

BOVA, S., GOLDMAN, W.F., YUAN, X.-J. & BLAUSTEIN, M.P. (1990). Influence of Na^+ gradient on Ca^{2+} transients and contraction in vascular smooth muscle. *Am. J. Physiol.,* **259,** H409–H423.

BRENNER, R., PERÉZ, G.J., BONEV, A.D., ECKMAN, D.M., KOSEK, J.C., WILER, S.W., PATTERSON, A.J., NELSON, M.T. & ALDRICH, R.W. (2000). Vasoregulation by the β_1 subunit of the calcium-activated potassium channel. *Nature,* **407,** 870–876.

BRUSCHI, G., BRUSCHI, M.E., REGOLISTI, G. & BORGHETTI, A. (1988). Myoplasmic Ca^{2+}-force relationship studied with fura-2 during stimulation of rat aortic smooth muscle. *Am. J. Physiol.,* **254,** H840–H854.

BYCHKOV, R., GOLLASCH, M., STEINKE, T., RIED, C., LUFT, F.C. & HALLER, H. (1998). Calcium-activated potassium channels and nitrate-induced vasodilation in human coronary arteries. *J. Pharmacol. Exp. Ther.,* **285,** 293–298.

CHEN, G. & SUZUKI, H. (1989). Some electrical properties of the endothelium-dependent hyperpolarization recorded from rat arterial smooth muscle cells. *J. Physiol.,* **410,** 91–106.

CHEN, X.L. & REMBOLD, C.M. (1995). Phenylephrine contracts rat tail artery by one electromechanical and three pharmacomechanical mechanisms. *Am. J. Physiol.,* **268,** H74–H81.

CHEONG, A., DEDMAN, A.M. & BEECH, D.J. (2001a). Expression and function of native potassium channel $[K_V\alpha1]$ subunits in terminal arterioles of rabbit. *J. Physiol.,* **534,** 691–700.

CHEONG, A., DEDMAN, A.M., XU, S.Z. & BEECH, D.J. (2001b). $K_V\alpha1$ channels in murine arterioles: differential cellular expression and regulation of diameter. *Am. J. Physiol.,* **281,** H1057–H1065.

CHEONG, A., QUINN, K., DEDMAN, A.M. & BEECH, D.J. (2002). Activation thresholds of K_V, BK and Cl_{Ca} channels in smooth muscle cells in pial precapillary arterioles. *J. Vasc. Res.,* **39,** 122–130.

COOK, N.S. (1989). Effect of some potassium channel blockers on contractile responses of the rabbit aorta. *J. Cardiovasc. Pharmacol.,* **13,** 299–306.

COPPOCK, E.A., MARTENS, J.R. & TAMKUN, M.M. (2001). Molecular basis of hypoxia-induced pulmonary vasoconstriction: role of voltage-gated K^+ channels. *Am. J. Physiol.,* **281,** L1–L12.

COX, R.H., FOLANDER, K. & SWANSON, R. (2001). Differential expression of voltage-gated K^+ channel genes in arteries from spontaneously hypertensive and Wistar–Kyoto rats. *Hypertension,* **37,** 1315–1322.

DAVIES, A.R. & KOZLOWSKI, R.Z. (2001). Kv channel subunit expression in rat pulmonary arteries. *Lung,* **179,** 147–161.

DOI, S., DAMRON, D.S., OGAWA, K., TANAKA, S., HORIBE, M. & MURRAY, P.A. (2000). K^+ channel inhibition, calcium signaling, and vasomotor tone in canine pulmonary artery smooth muscle. *Am. J. Physiol.,* **279,** L242–L251.

DORA, K.A., HINTON, J.M., WALKER, S.D. & GARLAND, C.J. (2000). An indirect influence of phenylephrine on the release of endothelium-derived vasodilators in rat small mesenteric artery. *Br. J. Pharmacol.,* **129,** 381–387.

ENGLAND, S.K., WOOLDRIDGE, T.A., STEKIEL, W.J. & RUSCH, N.J. (1993). Enhanced single-channel K^+ current in arterial membranes from genetically hypertensive rats. *Am. J. Physiol.,* **264,** H1337–H1345.

FELIX, J.P., BUGIANESI, R.M., SCHMALHOFER, W.A., BORRIS, R., GOETZ, M.A., HENSENS, O.D., BAO, J.M., KAYSER, F., PARSONS, W.H., RUPPRECHT, K., GARCIA, M.L., KACZOROWSKI, G.J. & SLAUGHTER, R.S. (1999). Identification and biochemical characterization of a novel nortriterpene inhibitor of the human lymphocyte voltage-gated potassium channel, Kv1.3. *Biochemistry,* **38,** 4922–4930.

FREEMAN, K.A., MAO, A., NORDBERG, L.O., PAK, J. & TALLARIDA, R.J. (1995). The relationship between vessel wall tension and the magnitude and frequency of oscillation in rat aorta. *Life Sci.,* **56,** PL129–PL134.

GELBAND, C.H. & HUME, J.R. (1995). $[Ca^{2+}]_i$ inhibition of K^+ channels in canine renal artery. Novel mechanism for agonist-induced membrane depolarization. *Circ. Res.,* **77,** 121–130.

GOKINA, N.I., WELLMAN, T.D., BEVAN, R.D., WALTERS, C.L., PENAR, P.L. & BEVAN, J.A. (1996). Role of Ca^{2+}-activated K^+ channels in the regulation of membrane potential and tone of smooth muscle in human pial arteries. *Circ. Res.,* **79,** 881–886.

GOLLASCH, M., WELLMAN, G.C., KNOT, H.J., JAGGAR, J.H., DAMON, D.H., BONEV, A.D. & NELSON, M.T. (1998). Ontogeny of local sarcoplasmic reticulum Ca^{2+} signals in cerebral arteries: Ca^{2+} sparks as elementary physiological events. *Circ. Res.,* **83,** 1104–1114.

GRISSMER, S., NGUYEN, A.N., AIYAR, J., HANSON, D.C., MATHER, R.J., GUTMAN, G.A., AUPERIN, D.D. & CHANDY, K.G. (1994). Pharmacological characterization of five cloned voltage-gated K^+ channels, types Kv1.1, 1.2, 1.3, 1.5, and 3.1, stably expressed in mammalian cell lines. *Mol. Pharmacol.,* **45,** 1227–1234.

GUSTAFSSON, H. (1993). Vasomotion and underlying mechanisms in small arteries. An *in vitro* study of rat blood vessels. *Acta Physiol. Scand.,* **614** (Suppl.), 1–44.

HANNER, M., SCHMALHOFER, W.A., GREEN, B., BORDALLO, C., LIU, J., SLAUGHTER, R.S., KACZOROWSKI, G.J. & GARCIA, M.L. (1999). Binding of correolide to K_{v1} family potassium channels. Mapping the domains of high affinity interaction. *J. Biol. Chem.,* **274,** 25237–25244.

HAYASHIDA, N., OKUI, K. & FUKUDA, Y. (1986). Mechanism of spontaneous rhythmic contraction in isolated rat large artery. *Jpn. J. Physiol.,* **36,** 783–794.

JACKSON, W.F. & BLAIR, K.L. (1998). Characterization and function of Ca^{2+}-activated K^+ channels in arteriolar muscle cells. *Am. J. Physiol.,* **274,** H27–H34.

JAGGAR, J.H., WELLMAN, G.C., HEPPNER, T.J., PORTER, V.A., PEREZ, G.J., GOLLASCH, M., KLEPPISCH, T., RUBART, M., STEVENSON, A.S., LEDERER, W.J., KNOT, H.J., BONEV, A.D. & NELSON, M.T. (1998). Ca^{2+} channels, ryanodine receptors and Ca^{2+}-activated K^+ channels: a functional unit for regulating arterial tone. *Acta Physiol. Scand.,* **164,** 577–587.

JIANG, J., THOREN, P., CALIGIURI, G., HANSSON, G.K. & PERNOW, J. (1999). Enhanced phenylephrine-induced rhythmic activity in the atherosclerotic mouse aorta *via* an increase in opening of K_{Ca} channels: relation to K_v channels and nitric oxide. *Br. J. Pharmacol.,* **128,** 637–646.

KHAN, R.N., SMITH, S.K., MORRISON, J.J. & ASHFORD, M.L. (1997). Ca^{2+} dependence and pharmacology of large-conductance K^+ channels in nonlabor and labor human uterine myocytes. *Am. J. Physiol.,* **273,** C1721–C1731.

KIYOSHI, A., ISHIKAWA, T., HAYASHI, K., IWATSUKI, Y., ISHII, K. & NAKAYAMA, K. (2003). Rhythmical contractions in pulmonary arteries of monocrotaline-induced pulmonary hypertensive rats. *Pflügers Arch.,* **447,** 142–149.

KNOT, H.J. & NELSON, M.T. (1998). Regulation of arterial diameter and wall $[Ca^{2+}]$ in cerebral arteries of rat by membrane potential and intravascular pressure. *J. Physiol.,* **508,** 199–209.

KNOT, H.J. & NELSON, M.T. (1995). Regulation of membrane potential and diameter by voltage-dependent K^+ channels in rabbit myogenic cerebral arteries. *Am. J. Physiol.,* **269,** H348–H355.

KRAMER, J.W., POST, M.A., BROWN, A.M. & KIRSCH, G.E. (1998). Modulation of potassium channel gating by coexpression of Kv2.1 with regulatory Kv5.1 or Kv6.1 α-subunits. *Am. J. Physiol.,* **274,** C1501–C1510.

LANGTON, P.D., NELSON, M.T., HUANG, Y. & STANDEN, N.B. (1991). Block of calcium-activated potassium channels in mammalian arterial myocytes by tetraethylammonium ions. *Am. J. Physiol.,* **260,** H927–H934.

LI, G. & CHEUNG, D.W. (1999). Effects of paxilline on K^+ channels in rat mesenteric arterial cells. *Eur. J. Pharmacol.,* **372,** 103–107.

LIU, Y., HUDETZ, A.G., KNAUS, H.G. & RUSCH, N.J. (1998). Increased expression of Ca^{2+}-sensitive K^+ channels in the cerebral microcirculation of genetically hypertensive rats: evidence for their protection against cerebral vasospasm. *Circ. Res.,* **82,** 729–737.

LONG, W., ZHANG, L. & LONGO, L.D. (2000). Cerebral artery K_{ATP}- and K_{Ca}-channel activity and contractility: changes with development. *Am. J. Physiol.,* **279,** R2004–R2014.

MILESI, V., AIELLO, E.A., REBOLLEDO, A., GOMEZ, A.A. & GRASSI DE GENDE, A.O. (1999). Role of a Ca^{2+}-activated K^+ current in the maintenance of resting membrane potential of isolated, human, saphenous vein smooth muscle cells. *Pflügers Arch.,* **437,** 455–461.

MULVANY, M.J., NILSSON, H. & FLATMAN, J.A. (1982). Role of membrane potential in the response of rat small mesenteric arteries to exogenous noradrenaline stimulation. *J. Physiol.,* **332,** 363–373.

NELSON, M.T., PATLAK, J.B., WORLEY, J.F. & STANDEN, N.B. (1990). Calcium channels, potassium channels, and voltage dependence of arterial smooth muscle tone. *Am. J. Physiol.,* **259,** C3–C18.

NELSON, M.T. & QUAYLE, J.M. (1995). Physiological roles and properties of potassium channels in arterial smooth muscle. *Am. J. Physiol.,* **268,** C799–C822.

NOGUERA, M.A., MADRERO, Y., IVORRA, M.D. & D'OCON, P. (1998). Characterization of two different Ca^{2+} entry pathways dependent on depletion of internal Ca^{2+} pools in rat aorta. *Naunyn Schmiedeberg's Arch. Pharmacol.,* **357,** 92–99.

OISHI, H., SCHUSTER, A., LAMBOLEY, M., STERGIOPULOS, N., MEISTER, J.J. & BÉNY, J.L. (2002). Role of membrane potential in vasomotion of isolated pressurized rat arteries. *Life Sci.,* **71,** 2239–2248.

PAPAGEORGIOU, P. & MORGAN, K.G. (1991). Intracellular free Ca^{2+} is elevated in hypertrophic aortic muscle from hypertensive rats. *Am. J. Physiol.,* **260,** H507–H515.

PASCUAL, J.M., SHIEH, C.C., KIRSCH, G.E. & BROWN, A.M. (1997). Contribution of the NH_2 terminus of Kv2.1 to channel activation. *Am. J. Physiol.,* **273,** C1849–C1858.

PENG, H.L., JENSEN, P.E., NILSSON, H. & AALKJÆR, C. (1998). Effect of acidosis on tension and $[Ca^{2+}]_i$ in rat cerebral arteries: is there a role for membrane potential? *Am. J. Physiol.,* **274,** H655–H662.

PÉREZ, G.J., BONEV, A.D. & NELSON, M.T. (2001). Micromolar Ca^{2+} from sparks activates Ca^{2+}-sensitive K^+ channels in rat cerebral artery smooth muscle. *Am. J. Physiol.,* **281,** C1769–C1775.

PLÜGER, S., FAULHABER, J., FÜRSTENAU, M., LÖHN, M., WALDSCHÜTZ, R., GOLLASCH, M., HALLER, H., LUFT, F.C., EHMKE, H. & PONGS, O. (2000). Mice with disrupted BK channel β1 subunit gene feature abnormal Ca^{2+} spark/STOC coupling and elevated blood pressure. *Circ. Res.,* **87,** E53–E60.

POST, M.A., KIRSCH, G.E. & BROWN, A.M. (1996). Kv2.1 and electrically silent Kv6.1 potassium channel subunits combine and express a novel current. *FEBS Lett.,* **399,** 177–182.

ROBERDS, S.L. & TAMKUN, M.M. (1991). Cloning and tissue-specific expression of five voltage-gated potassium channel cDNAs expressed in rat heart. *Proc. Natl. Acad. Sci. U.S.A.,* **88,** 1798–1802.

SADOSHIMA, J., AKAIKE, N., TOMOIKE, H., KANAIDE, H. & NAKAMURA, M. (1988). Ca-activated K channel in cultured smooth muscle cells of rat aortic media. *Am. J. Physiol.,* **255,** H410–H418.

SANSOM, S.C. & STOCKAND, J.D. (1994). Differential Ca^{2+} sensitivities of BK(Ca) isochannels in bovine mesenteric vascular smooth muscle. *Am. J. Physiol.,* **266,** C1182–C1189.

SEIDEN, J.E., PLATOSHYN, O., BAKST, A.E., MCDANIEL, S.S. & YUAN, J.X. (2000). High K^+-induced membrane depolarization attenuates endothelium-dependent pulmonary vasodilation. *Am. J. Physiol.,* **278,** L261–L267.

SHIMA, H. & BLAUSTEIN, M.P. (1992). Modulation of evoked contractions in rat arteries by ryanodine, thapsigargin, and cyclopiazonic acid. *Circ. Res.,* **70,** 968–977.

SHIMAMURA, K., SEKIGUCHI, F. & SUNANO, S. (1999). Tension oscillation in arteries and its abnormality in hypertensive animals. *Clin. Exp. Pharmacol. Physiol.,* **26,** 275–284.

SHIMIZU, S., YOKOSHIKI, H., SPERELAKIS, N. & PAUL, R.J. (2000). Role of voltage-dependent and Ca^{2+}-activated K^+ channels on the regulation of isometric force in porcine coronary artery. *J. Vasc. Res.,* **37,** 16–25.

SMIRNOV, S.V. & AARONSON, P.I. (1994). Alteration of the transmembrane K^+ gradient during development of delayed rectifier in isolated rat pulmonary arterial cells. *J. Gen. Physiol.,* **104,** 241–264.

SMIRNOV, S.V., BECK, R., TAMMARO, P., ISHII, T. & AARONSON, P.I. (2002). Electrophysiologically distinct smooth muscle cell subtypes in rat conduit and resistance pulmonary arteries. *J. Physiol.,* **538,** 867–878.

SMIRNOV, S.V., ROBERTSON, T.P., WARD, J.P.T. & AARONSON, P.I. (1994). Chronic hypoxia is associated with reduced delayed rectifier K^+ current in rat pulmonary artery muscle cells. *Am. J. Physiol.,* **266,** H365–H370.

TAMMARO, P., AARONSON, P.I. & SMIRNOV, S.V. (2001). Modulation of the native Kv2.1 channel by phosphorylation in rat aortic myocytes. *Biophys. J.,* **80** (Part 2), 440a.

TAMMARO, P. & SMIRNOV, S.V. (2002). Modulation of K_v channel currents by bisindolylmaleimide I (BIM), a selective PKC, inhibitor, in rat aortic myocytes. *Biophys. J.,* **82** (Part 2), 285A.

TAMMARO, P. & SMIRNOV, S.V. (2003). Modulation of the voltage-gated potassium (K_v) channel currents by intracellular Mg^{2+} in rat aortic smooth muscle cells (RASMCs). *J. Physiol.,* **547.P,** C47.

TANAKA, Y., MEERA, P., SONG, M., KNAUS, H.G. & TORO, L. (1997). Molecular constituents of maxi K_{Ca} channels in human coronary smooth muscle: predominant $\alpha+\beta$ subunit complexes. *J. Physiol.,* **502,** 545–557.

THORNE, G.D., CONFORTI, L. & PAUL, R.J. (2002). Hypoxic vasorelaxation inhibition by organ culture correlates with loss of Kv channels but not Ca^{2+} channels. *Am. J. Physiol.,* **283,** H247–H253.

TOSUN, M., PAUL, R.J. & RAPOPORT, R.M. (1998). Coupling of store-operated Ca^{2+} entry to contraction in rat aorta. *J. Pharmacol. Exp. Ther.,* **285,** 759–766.

UCHIDA, Y., NAKAMURA, F., TOMARU, T., SUMINO, S., KATO, A. & SUGIMOTO, T. (1986). Phasic contractions of canine and human coronary arteries induced by potassium channel blockers. *Jpn. Heart J.,* **27,** 727–740.

WESSELMAN, J.P., SCHUBERT, R., VANBAVEL, E.D., NILSSON, H. & MULVANY, M.J. (1997). K_{Ca}-channel blockade prevents sustained pressure-induced depolarization in rat mesenteric small arteries. *Am. J. Physiol.,* **272,** H2241–H2249.

(Received April 30, 2004
Revised July 1, 2004
Accepted July 15, 2004)